Coupling the modeling of phage-bacteria interaction and cholera epidemiological model with and without optimal control

Hyacinthe M. Ndongmo Teytsa[a,c] **Berge Tsanou**[a,b,c,1] **Samuel Bowong**[c,d] **Jean Lubuma**[b]

[a] *Research Unit for Mathematics and Applications, Department of Mathematics and Computer Science, University of Dschang, P.O. Box 67 Dschang, Cameroon.*
[b] *Department of Mathematics and Applied Mathematics, University of Pretoria, Pretoria 0002, South Africa*
[c] *IRD UMI 209 UMMISCO, University of Yaounde I, P.O. Box 337 Yaounde, Cameroon and LIRIMA-EPITAG Team Project, University of Yaounde I, P.O. Box 812 Yaounde, Cameroon*
[d] *Department of Mathematics and Computer Science, University of Douala, P.O. Box 24157, Cameroon*

Abstract

In this work, we assess the impact of the phage-bacteria infection and optimal control on the indirectly transmitted cholera disease. The phage-bacteria interactions are described by predator-prey system using the Smith functional response, which takes into account the number of bacteria binding sites. The study is done in two steps, namely the model without control and the model with control. For the first scenario, we explicitly compute the basic reproduction number $\mathcal{R}_0$ which serves as stability threshold and bifurcation parameter. The proposed model exhibits a bi-stability phenomenon via the existence of backward bifurcation, which implies that the classical requirement of bringing the reproduction number under unity, while necessary, is no longer sufficient for cholera elimination from the population. We intuitively introduce a new threshold number $\mathcal{N}_0$ needed for the global stability of the disease free equilibrium point which is achieved when $R_0 \leq 1$ and $\mathcal{N}_0 \leq 1$. It is further shown that the phage absorption is a possible cause of bi-stability, since in its absence, the condition $\mathcal{R}_0 \leq 1$ is sufficient for cholera to die out. The existence of endemic equilibrium points depends on the range of both $\mathcal{R}_0$ and $\mathcal{N}_0$. Regarding the model extended to an optimal control problem, which involves the use of virulent vibriophages to reduce or eliminate the bacteria population, we use optimal control theory techniques. We establish the conditions under which the spread of cholera can be stopped, and examine the impact of control measures on the transmission dynamic of cholera. The Pontryagin's maximum principle is used to characterize the optimal control. Numerical simulations suggest that, the release of lytic vibriophages can significantly reduce the spread of the disease. We discuss opportunities for phage therapy as treatment of some bacterial-borne diseases without side effects.

Keywords: Bi-stability, Optimal control, Smith attachment function, Bifurcation, Virulent phage, Phage absorption.

1. Introduction

Cholera is commonly known as the "*disease of dirty hands*". It is an infection of the small intestine caused by some strains of the vibrio cholerae. The two ecological serogroups (Vibrio cholerae 01 and Vibrio cholera 0139) have the ability to colonize the hosts small intestine. It may happen that symptoms are not visible, but when they arise, one notices high dehydration of the infected person through watery diarrhea that lasts a few days. This may result in sunken eyes, cold skin, decreased skin elasticity, and wrinkling of hands and feet. Symptoms start two hours to five days after exposure. Cholera affects an estimated 3-5 million people worldwide and causes 28,800-130,000 deaths *per* year [56, 57]. As of

[1] *Corresponding author*: Berge Tsanou, E-mail: berge.tsanou@up.ac.za / berge.tsanou@univ-dschang.org

2010, cholera has been classified as a pandemic disease, though it is rare in developed countries. The most affected people are children, especially in Africa and Southeast Asia. The usual fatality rate of cholera is less than 5%, but this can dramatically reach 50% in some areas where access to treatment is unavailable. Vibrio Cholerae can survive in some aquatic environment for three months to two years. Typically, these viruses live in association with zoo-plankton, phytoplankton and the aquatic organism such as bacteriophages [57].

Phages or bacteriophages, also known as viruses for bacteria, are parasites which replicate only when they infect bacteria. They are the most populated organisms in the aquatic ecosystem and probably in the world. As parasites, their survival and multiplication depend on the existence of specific types of bacteria they can infect. Based on their survival strategies, phages exhibit the following three different life cycles: lytic, lysogenic and pseudo-lysogenic [15]. In its lytic life cycle, a phage injects a bacterium cell and multiplies such that new phages burst from the cell and kill the bacterium. In the lysogenic cycle, the phage does not replicate but becomes a prophage whereby its genome goes into a quiescent condition where it is usually integrated into the host genome or alternatively it is maintained as an extra chromosomal plasmid [15]. During the lysogenic life cycle, the host cell survives and continues to reproduce with the virus being reproduced in all daughter cells. In the pseudo-lysogenic life cycle, the phage neither undergoes lysogeny nor shows lytic cycle; but it remains inactive. There is a class of phages which are restricted to either the lytic or lysogenic cycle. Phages that replicate only via the lytic cycle are known as virulent phages, while those that replicate using both lytic and lysogenic cycles are known as temperate phages. In the lysogenic cycle, upon detection of cell damage, such as ultra-violet radiation light or certain chemical, the prophage is extracted from the bacterial chromosome in a process called prophage induction [7]. After induction, viral replication begins via the lytic cycle.

The presence of phages in an environmental reservoir plays an essential role in the evolution of bacterial species. Therefore, the interaction between phages and bacteria can trigger some environmental indirect transmitted diseases by enabling the emergence of new clones of virulent pathogenic bacteria. For instance, when infected by temperate phages, Vibrio cholerae evolve from environmental non-pathogenic strains to highly pathogenic species by acquisition of virulent genes through the lysogenic cycle in the phage-bacteria interaction [15]. Furthermore, the presence or introduction of virulent phages in the environment or in the human guts can help to combat or treat cholera. Thus, understanding the genetic and ecological factors, which support the phage-bacteria interaction, the production of highly virulent pathogenic species, and the presence of virulent lytic phages is essential to develop preventive measures for environment-borne diseases such as cholera. In this regard, mathematical modeling is an important tool to provide insights into the co-evolution or extinction of bacteria and phages.

Several studies have been carried out on the phage bacterial interactions from both the mathematical [37, 49, 50, 51], and the biological [7, 9, 15, 20, 23, 24, 40] perspectives. The majority of these works dealt with the description of the lytic cycle of phages and the use of virulent phages to control infection and bacterial contamination. Few of them have been devoted to the lysogenic cycle, prophage induction and the proliferation of pathogenic bacteria due to phage-bacteria infection. Recently, Hal Smith [49] proposed a mathematical model of virulent phage growth with application to phage therapy. The novelty in this work was the consideration of a new functional response, which takes into account the number of binding sides as well as the explicit modeling of the loss of phages due to attachment.

The general setting of this paper is a cholera epidemiological model. We build on, and extend some of the existing works in the literature in the following three directions:

(i) We consider the bacteria interaction with phages (lytic and temperate).

(ii) We use the phage-bacteria functional response similar to the one proposed by Smith [49].

(iii) In order to control the proliferation of pathogenic bacteria, the model is further extended to an optimal control problem by adding a class of selected virulent phages that are continuously released into the environment.

Our methodology is twofold. Firstly, we formulate a model without control. The basic reproduction number $\mathcal{R}_0$ is computed, and the existence and stability of equilibrium points are investigated. We prove that the disease free equilibrium point (DFE) is locally asymptotically stable whenever $\mathcal{R}_0 < 1$. The system exhibits a bi-stability phenomenon via the existence of backward bifurcation due to the phage absorption. This implies that the classical epidemiological requirement for effective elimination of cholera, $\mathcal{R}_0 < 1$, is no longer sufficient. Due to the existence of backward bifurcation, we determine another threshold $\mathcal{N}_0$, such that the DFE is globally asymptotically stable when both $\mathcal{R}_0$ and $\mathcal{N}_0$ are less than one, irrespective of their order of comparison. On the other hand, depending on the range of $\mathcal{R}_0$ and $\mathcal{N}_0$, the proposed model can exhibit one or more endemic equilibrium points. In the absence of the phage absorption, so that there is no backward bifurcation, the model exhibits a trans-critical forward bifurcation at $\mathcal{R}_0 = 1$. Precisely, it is proven that there is no endemic equilibrium point whenever $\mathcal{R}_0 < 1$, while there exists a unique globally asymptotically stable endemic equilibrium point whenever $\mathcal{R}_0 > 1$.

Secondly, we formulate an optimal control problem assuming the release of selected virulent phages as a strategy for elimination of cholera disease. Notice that the virulent phages selection is possible using the methods in [24, 40]. The theoretical analysis and numerical simulations of the control model show that, in the presence of virulent phages shed into environment, the population of susceptible humans increases, while the population of infected humans decreases significantly.

The rest of the paper is organized as follows. Section 2 is devoted to the model without control. We formulate it, study its basic properties, the bi-stability occurrence via bifurcation analysis, and provide the numerical simulations. While Section 3 deals with the formulation, analysis and numerical simulations of the optimal control problem, concluding remarks and discussions are given Section 4.

2. Model without control

2.1. Model derivation

Our model is in the framework of multi-hosts modeling, whereby the dynamics of the three interacting distinct populations of bacteria, phages and human beings is described, with the particularity that phages prey on bacteria. In the presence of phages or viruses denoted by P, the bacterium population splits into the following three classes: susceptible bacteria (not yet attacked by phages), lysogen bacteria (bacteria infected by temperate phages) and those infected by virulent phages.

Let B denote the susceptible or uninfected bacteria. They are free-living cholera agents capable of self multiplication in the environment. For simplicity, we assume that their growth rate is a constant r. Following the approach in [49], we argue that the phage attack rate or the phage-bacteria functional response and the rate of phage loss due to attachment are distinct. We recall that, the functional response is the number of prey successfully attacked per predator as a function of prey density. We model the phage-bacteria functional response by

$$h(B,P) = \varepsilon \frac{BP}{F_n(cP)}. \tag{2.1}$$

Here, ε is the absorption rate, and $c = \varepsilon/\rho$ with $1/\rho$, representing the injection time, *i.e.* the time between binding of phages to host bacteria and subsequent injection of genetic material into host, and n denotes the number of binding sites for phages per host (bacterium). The function $f(P)$

$$f(P) = \frac{P}{F_n(cP)}, \tag{2.2}$$

is the phage attack rate proposed in [49], where

$$F_n(P) = 1 + \frac{P}{1+P} + \frac{P^2}{(1+P)(2+P)} + ... + \frac{P^n}{(1+P)(2+P)...(n-1+P)n}. \tag{2.3}$$

The following properties of f and F_n are derived from Lemma 2.1 in [49]:

1. $\frac{d}{dP}F_n(P) > 0$ and $\frac{d}{dP}f(P) > 0$.

2. $\lim_{P\to+\infty} f(P) = n$.

3. $F_n(P) > 1$.

4. $F_\infty(P) \leq F_{n+1}(P) \leq F_n(P) \leq F_1(P) = 1 + P$.

For the numerical simulations, we shall choose $n = 3$. This choice is not a severe limitation, as $F_n(P)$ depends rather weakly on n and $F_3(P)$ is a good approximation of $F_{100}(P)$ on $0 < P < 5$ [49].

We assume that the bacteria population cannot maintain itself through growth in the environment. Thus, the decay rate μ_b of bacteria is greater than r. It is known that multiple phage infection is not possible. Thus, susceptible bacteria are infected either by temperate or virulent phages. We denote by π the proportion of lysogen bacteria and $1 - \pi$ the proportion of bacteria infected by virulent phages.

Let B_T denote the lysogen bacteria. The lysogenic cycle allows the host cell to continue to survive and reproduce, the virus is reproduced in all of the cell's offspring. The genetic material of phages called prophages can be transmitted to daughter cells at each subsequent cell division [7]. We denote the cell multiplication size by ϕ. In the course of cell division, the effect of ultra-violet radiations or the presence of certain chemicals can lead to the release of prophages causing proliferation of new phages through the process called prophage induction. Therefore, with α denoting the induction rate, αB_T is the number of lysogen bacteria that switch from a lysogenic cycle to a lytic cycle.

Let B_V denote the population of bacteria infected by virulent/lytic phage. In the lytic cycle, bacteria cells are broken (lysed) and destroyed after immediate replication of the new phages [7]. We denote by θ, the burst size of the bacteria and γ the bacteria death due to lysis.

With P the population of phages, we associate μ_P, the phage decay rate. The loss of phages may be significant during the phage-bacteria interactions. For example, if we assume that a phage cannot detect the state (uninfected or infected) of the host cell to which it binds, then one should not ignore the loss of the phage due to wasted attacks on already infected hosts [49]. We take into account the fact that a host cell has a multiplicity of potential phage binding sites on its surface, higher than the one that may be simultaneously bound by phage. Thus the rate of phage loss due to attachment can be described by the expression

$$-\varepsilon(B + B_T + B_V)P. \tag{2.4}$$

As far as the human total population at time t, $N \equiv N(t)$ is concerned, we split it into susceptible ($S \equiv S(t)$) and infected ($I \equiv I(t)$) compartments so that $N(t) = S(t) + I(t)$. We model the cholera epidemic by an SIS-W system, where W stands for the density of vibrio cholerae in the environment. Note that in this setting, vibrio cholerae play the role of bacteria and phages under consideration are those that infect vibrio cholerae also known as vibriophages. The recruitment rate in human population is constant and denoted by Λ. Human die naturally at the rate μ_h, while the death rate due to cholera is denoted by d and the recovered rate is δ. The phages can convert their bacterial hosts from non pathogenic strains to pathogenic strains through a process called phage conversion, by providing the hosts with phage-encoded virulence genes. Toxigenic vibrio cholerae isolates carry the ctxAB genes encoded by lysogenic phages. Thus, the susceptible human population acquire an infection by consuming the lysogen bacteria, at rate $\beta B_T S$ where β is the contact rate with environment. On the other hand, when the susceptible vibrio cholerae are ingested from the environment and reach the small intestine within the human body, then complex biological interactions, chemical reactions, and genetic transduction take place, which lead to human cholera [51]. The ingestion of susceptible vibrio cholerae can cause infection at rate $\beta k B$, where k is the infection rate of susceptible bacteria by temperate phages in the small intestine. The ingestion of infected bacteria B_V cannot lead to the infection since they are lysed to produce phages. Unlike [49], we have neglected the delay between the time vibrio cholera is infected and the moment it lyses. Thus, the force of infection is given by

$$\lambda = \beta(B_T + kB). \tag{2.5}$$

Symbols	Biological definitions	Baseline value	Range	Source
r	Intrinsic bacteria growth rate	0.8	$0.3 - 14.3$	[28]
μ_b	Bacteria decay rate	0.002	0-1	assumed
ω, η, ν	Bacteria shedding rates	20	10-100	[38]
ε	Phage absorption rate	0.0015	0-0.0025	[28, 49]
α	Prophage induction rate	0.4	$0.001 - 0.99$	assumed
ϕ	Cell division size	80	$10 - 100$	assumed
π	Fraction of lysogen bacteria	0.2	$0 - 1$	[7]
γ	Bacteria death rate due to lysis	1	$0.1 - 1$	assumed
θ	Bacteria burst size	100	$80 - 100$	[28]
e	Phage shedding rate	0.15	$0.1 - 0.99$	assumed
Λ	Human recruitment rate	20	1-5000	assumed
μ_h	Human natural death rate	0.002	0-1	[38]
d	Human death rate due to cholera	0.00005	$0 - 0.99$	[33]
δ	Human recovery rate	0.5	0-1	assumed
k	Infection rate in the small intestine	0.15	$0.4 - 0.99$	assumed

Table 1: Variables and parameters for model system (2.6).

Human contamination of the water supply through infected feces (*i.e.* shedding) contributes to bacteria levels. Therefore, the shedding rates of susceptible bacteria (B), lysogen bacteria (B_T) and infected bacteria (B_V) are denoted by ω, η and ν respectively. The above discussed process of the construction of the model is schematized in Figure 1, while Table 1 summarizes the description of the model parameters. Based on the above formulation and assumptions, the model describing the cholera dynamics is given by the following deterministic system of nonlinear differential equations:

$$\begin{cases} \dfrac{dS}{dt} = \Lambda - \beta(B_T + kB)S - \mu_h S + \delta I, \\ \dfrac{dI}{dt} = \beta(B_T + kB)S - (\mu_h + d + \delta)I, \\ \dfrac{dB}{dt} = \omega I + rB - \varepsilon B f(P) - \mu_b B, \\ \dfrac{dB_T}{dt} = \eta I + \phi\pi\varepsilon B f(P) - (\mu_b + \alpha\gamma)B_T, \\ \dfrac{dB_V}{dt} = \nu I + (1-\pi)\varepsilon B f(P) - (\mu_b + \gamma)B_V, \\ \dfrac{dP}{dt} = eI + \theta\gamma B_V + \theta\alpha\gamma B_T - \varepsilon(B_T + B_V + B)P - \mu_P P. \end{cases} \tag{2.6}$$

Though this model is formulated for cholera epidemics, we stress that it can apply to other bacterial-borne diseases, for which the disease pathogen can interact with a specific phage and lyse such as E. Coli, Q fever, Pyomysitis, Eurysipelas [24].

2.2. *Analysis of the model*

The model (2.6) monitors changes in the populations (humans, phages, bacteria). For it to be epidemiologically meaningful, it is important to prove that to non-negative initial data, corresponds a

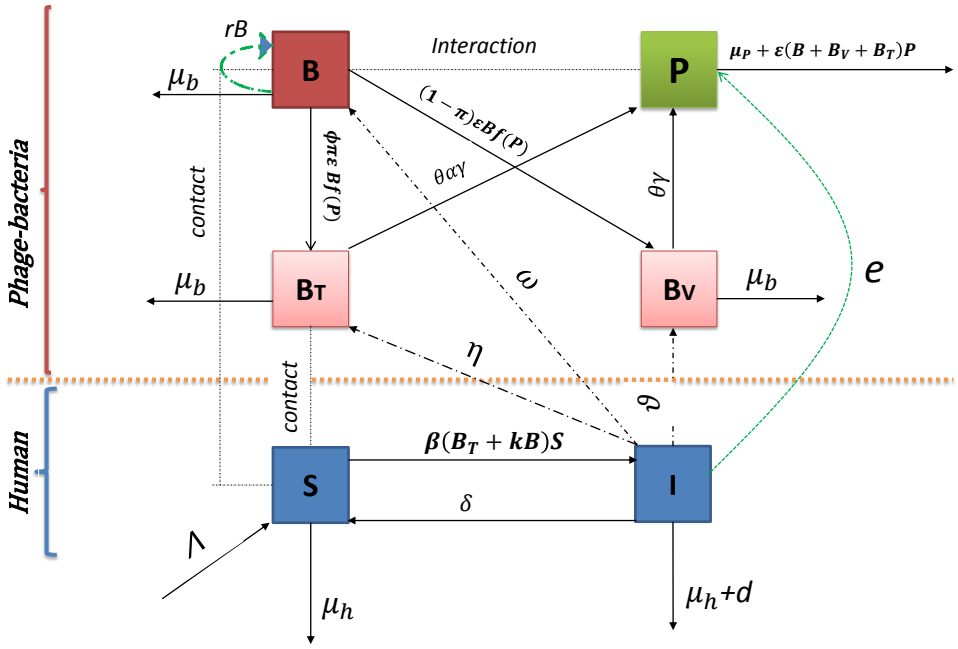

Figure 1: Simplified schematic flow diagram for model (2.6).

unique, bounded and non-negative solution for all $t \geq 0$. Set

$$N = S + I, \quad M = \phi B + B_T + \phi B_V, \quad M_m = \frac{\Lambda\phi(\omega + \eta + \nu)}{\mu_b\mu_h}, \quad P_m = \frac{\Lambda e}{\mu_h\mu_P} + \frac{\theta(\gamma + \alpha\gamma)M_m}{\mu_b\mu_h\mu_p}.$$

Then it is not difficult to prove the following result.

Theorem 2.1. *The model (2.6) is a dynamical system in the compact set*

$$\Omega = \left\{(S, I, B, B_T, B_V, P) \in \mathbb{R}^6_+, \ N(t) \leq \frac{\Lambda}{\mu_h}, \ M(t) \leq M_m, \ P(t) \leq P_m\right\}.$$

System (2.6) has a disease free equilibrium point given by $E_0 = (S_0, 0, 0, 0, 0, 0)$ with $S_0 = \Lambda/\mu_h$. The basic reproduction number of the model (2.6) is

$$\mathcal{R}_0 = \frac{\omega\beta k S_0}{(\mu_h + d + \delta)(\mu_b - r)} + \frac{\eta\beta S_0}{(\mu_h + d + \delta)(\mu_b + \alpha\gamma)}. \tag{2.7}$$

In (2.7), $\omega\beta k S_0/(\mu_h + d + \delta)(\mu_b - r)$ is the average number of secondary human infections produced by susceptible bacteria in their entire lifespan, while $\eta\beta S_0/(\mu_h + d + \delta)(\mu_b + \alpha\gamma)$ is the average number of secondary human infections produced by lysogen bacteria in their entire lifespan.

Proposition 2.2. *The diseases free equilibrium point E_0 is locally asymptotically stable (LAS) whenever $\mathcal{R}_0 < 1$ and unstable whenever $\mathcal{R}_0 > 1$.*

The proof of Proposition 2.2 is provided in Appendix A.

The biological implication of Proposition 2.2 is that, a sufficiently small flow of infectious individuals will not generate outbreak of the disease unless $\mathcal{R}_0 > 1$. For a better control on the disease, the global

asymptotic stability (GAS) of the DFE is needed. Note that, classically, the basic reproduction number of (2.6) $\mathcal{R}_0$ is the average number of secondary human infections through environmental transmission caused by infectious bacteria (B, B_T) during their entire lifespan. However, one should notice that $\mathcal{R}_0$ does not depend on the parameters of phage-bacteria interaction. This is not surprising, since system (2.6) couples an epidemic model (cholera) and a population dynamics model (predator-prey system). Usually, the in-depth asymptotic analysis of such a coupled system involves two thresholds, which for our model maybe: the epidemic threshold $\mathcal{R}_0$ and a coexistence threshold for the predator-prey system. The existence of the latter threshold for model (2.6) is actually expected because the infected human individuals contribute to the growth of bacteria. The threshold quantity $\mathcal{N}_0$ should actually be the average offspring number of lysogen bacteria produced, by one infected human during the phage-bacteria interaction. By inspection, we observe that, $\beta S_0/(\mu_h + d + \delta)$ is the average number of the infected individuals, $\left(\eta + \omega\phi\pi\right)$ is the rate of production lysogen bacteria either by shedding at rate η or by cell division at rate $\phi\pi\omega$, and $1/(\mu_b + \alpha\gamma)$ is the lysogen bacteria lifespan. Therefore, we define $\mathcal{N}_0$ by

$$\mathcal{N}_0 := \frac{\beta S_0}{\mu_h + d + \delta}\left(\eta + \omega\phi\pi\right)\frac{1}{\mu_b + \alpha\gamma}. \tag{2.8}$$

For further investigation, the threshold quantity $\mathcal{N}_0$ is used in the next theorem for the global asymptotic stability of the DFE, the proof of which is given in Appendix B.

Theorem 2.3. *The diseases free equilibrium point E_0 is globally asymptotically stable in Ω whenever $\mathcal{R}_0 \leq 1$ and $\mathcal{N}_0 \leq 1$.*

Theorem 2.3 indicates that regardless of the initial condition, cholera infection will ultimately die out as long as both the basic reproduction number $\mathcal{R}_0$ and the average offspring number of lysogen bacteria $\mathcal{N}_0$ are less than or equal to unity. Hence, affordable efforts should be made to bring both thresholds below unity. Contrary to most classical epidemiological models where, bringing only the basic reproduction number $\mathcal{R}_0$ below one is sufficient to eliminate the infection, more effort is needed here due the additional condition $\mathcal{N}_0 \leq 1$, which actually highlights the influence of the ecology of phages and bacteria on the cholera evolution. We perform a global sensitivity analysis to examine the model response to parameter variation within a wider range in parameter space. Following the approach in [42], Partial Rank Correlative Coefficient (PRCC) between $\mathcal{R}_0$, $\mathcal{N}_0$ and each parameter are derived. The results of the PRCC of $\mathcal{R}_0$ and $\mathcal{N}_0$ are shown in Figure 2. We observe that the parameters Λ, β, ω and η have the most positive influence on $\mathcal{R}_0$ and $\mathcal{N}_0$ (i.e increasing them), while those with most negative impact on $\mathcal{R}_0$ and $\mathcal{N}_0$ (i.e decreasing them) are μ_h, δ, α and μ_b. It is worth noting that $\mathcal{R}_0$ and $\mathcal{N}_0$ are similarly influenced by all the shared parameters.

In order to control the spread of cholera, some strategies can be implemented. For instance, it is proposed in [47] to reduce the contact rate β by informing people, and increasing the decay rate of bacteria μ_b through disinfection of contaminated environment. One may wish to assess how their combined action influence the basic reproduction number $\mathcal{R}_0$ and the threshold $\mathcal{N}_0$. Figure 3 is a bifurcation diagram which uses the curves of $\mathcal{R}_0 = 1$ and $\mathcal{N}_0 = 1$ to separate $\mathbb{R}^2_+$ into four regions. Figure 3 specifically shows that, for a couple $(\mu_b, \beta) \in D_0$, and fixing other parameters, cholera is eliminated. The global asymptotic stability of the DFE established in Theorem 2.3 is illustrated numerically on Figure 4, where the trajectories of model (2.6) are plotted for different initial conditions for $\mathcal{R}_0 = 0.7756$ and $\mathcal{N}_0 = 0.8049$. From Figure 4, we observe that the susceptible human population sustains , while infected human and the total population of infectious bacteria disappear.

2.2.1. Existence of endemic equilibrium points

An endemic point (EE) of model (2.6) is the state where infected humans, bacteria and phages cannot be totally eradicated but remain in the human population and environment. In this context we have three sub-populations and several infected compartments. Thus the single threshold $\mathcal{R}_0$ cannot be sufficient

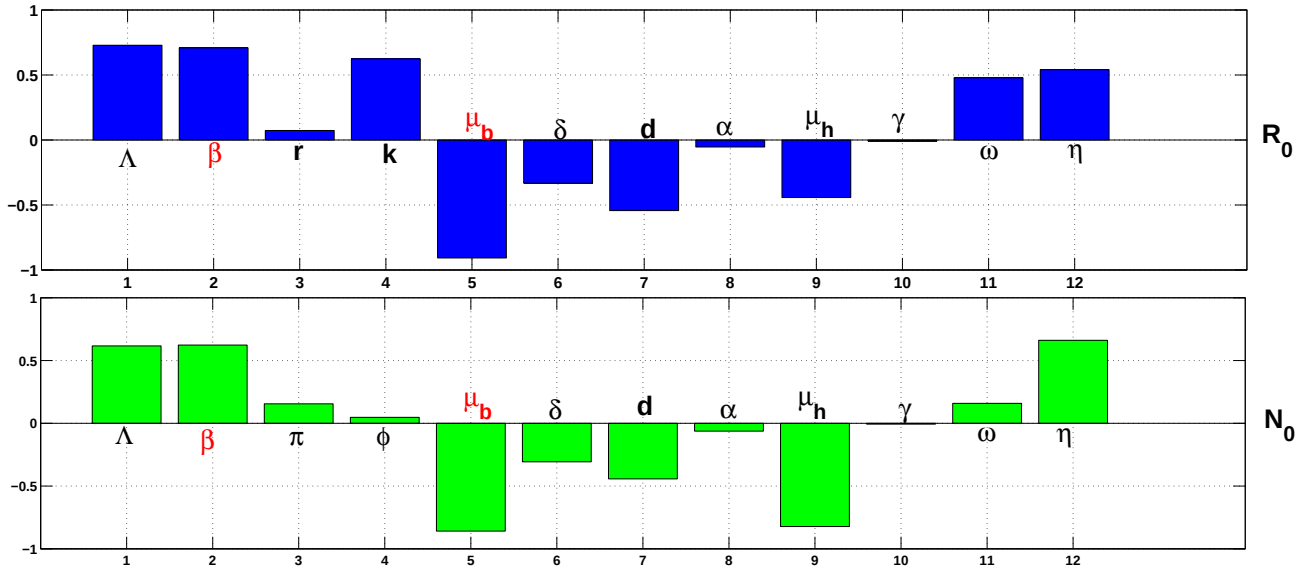

Figure 2: Sensitivity analysis and Partial Rank Correlation Coefficients (PRCC) for $\mathcal{R}_0$ and $\mathcal{N}_0$: The parameters in red color are the most influential. $\mathcal{R}_0$ and $\mathcal{N}_0$ are similarly influenced by all the shared parameters.

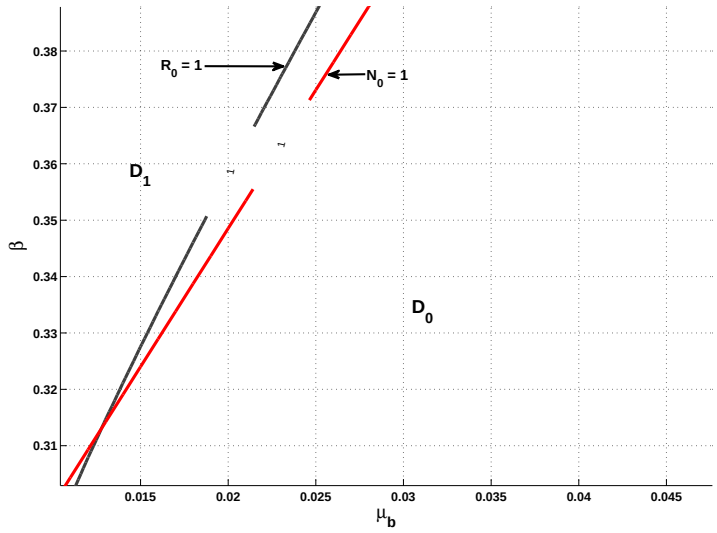

Figure 3: Contour plot of $\mathcal{R}_0$ and $\mathcal{N}_0$ in the (β, μ_b) plane.

to derive conditions for the existence of EE. In this section we highlight that, the existence of EE of model (2.6) depends on the epidemiological threshold $\mathcal{R}_0$ for human sub-system as well as the ecological threshold $\mathcal{N}_0$ for the phage-bacteria sub-system. The precise result is stated in the next theorem which is proved in Appendix C.

Theorem 2.4. *The following statements hold true:*
(i) The model (2.6) *has a unique endemic equilibrium point whenever* $\mathcal{R}_0 > 1$ *and* $\mathcal{N}_0 > 1$.
(ii) There is no endemic equilibrium point for model (2.6) *whenever* $\mathcal{R}_0 \leq 1$ *and* $\mathcal{N}_0 \leq 1$.

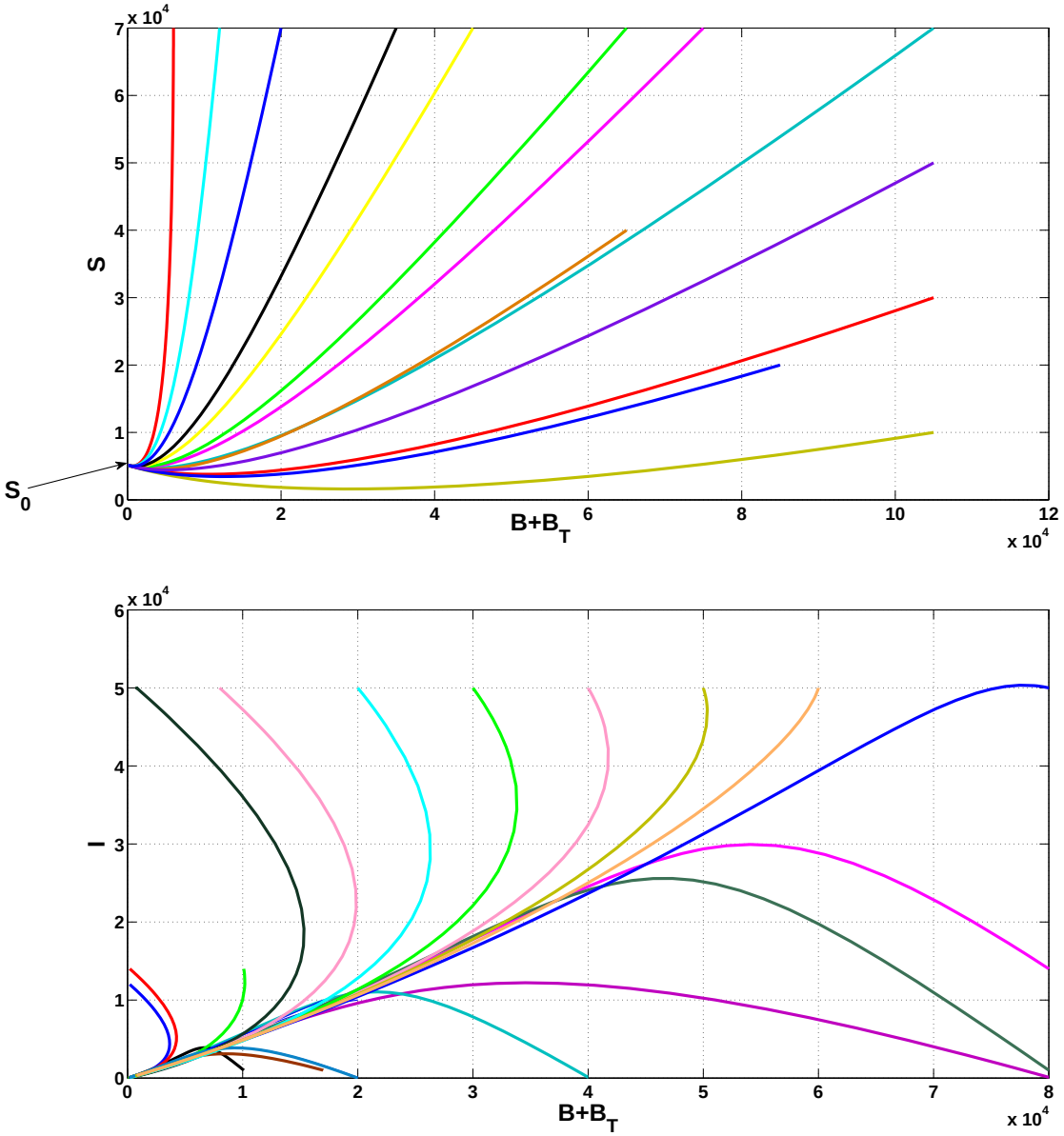

Figure 4: Global stability of E_0 with $\mathcal{R}_0 = 0.7756$ and $\mathcal{N}_0 = 0.8049$.

(iii) For the other cases, the model (2.6) *at least three endemic equilibrium points.*

2.3. *Bifurcation analysis*

While parts (*i*) and (*ii*) of Theorem 2.4 are clear, the dynamics in part (*iii*) needs to be unpacked as it suggests the existence of the bi-stability phenomenon. This is what we investigate in this section.

2.3.1. *Backward and forward Bifurcations*

To conduct the bifurcation analysis, we define the two following thresholds. The first one, β^* is obtained by setting $\mathcal{R}_0 = 1$ in (2.7)

$$\beta^* = \frac{(\mu_h + d + \delta)(\mu_b - r)(\mu_b + \alpha\gamma)}{\omega k(\mu_b + \alpha\gamma)S_0 + \eta(\mu_b - r)S_0}.$$

The second one, χ_0, is defined by

$$\chi_0 = 1 + \frac{\beta^*(\mu_h + d)\left(k\omega(\mu_b + \alpha\gamma) + \eta(\mu_b - r)\right)(\mu_b + \gamma)S_0}{\mu_h\theta\gamma(\mu_b + \gamma)\left((\mu_b + \gamma)\alpha + \mu_b + \alpha\gamma\right) + e(\mu_b + \alpha\gamma)(\mu_b + \gamma)}. \tag{2.9}$$

Theorem 2.5. *The model (2.6) exhibits the following types of bifurcations at $\mathcal{R}_0 = 1$:*

i) A forward (trans-critical) bifurcation whenever $1 < \mathcal{N}_0 < \chi_0$. That is the DFE is LAS whenever $\mathcal{R}_0 < 1$, becomes unstable whenever $\mathcal{R}_0 > 1$, and gives rise to a LAS endemic equilibrium point.

ii) A backward (sub-critical) bifurcation whenever $\mathcal{N}_0 > \chi_0$. That is there exits a LAS endemic equilibrium point when $\mathcal{R}_0 < 1$ which coexists with the LAS DFE.

The proof of Theorem 2.5 is provided in Appendix D, while the illustrative bifurcation diagrams are shown on Figures 5. To this is added the illustration of the bi-stability phenomenon in Figure 6 whenever $\mathcal{R}_0 = 0.1711$.

For the initial condition $(S_0, I_0, B_0, B_{T0}, B_{V0}, P_0) = (1000, 100, 10^3, 500, 100, 400)$, the solution converges the to disease-free equilibrium point, while for the initial condition $(S_0, I_0, B_0, B_{T0}, B_{V0}, P_0) = (1000, 100, 10^6, 5 \times 10^4, 100, 400)$ the corresponding solution tends rather to the endemic equilibrium point.

2.3.2. The cause of bi-stability

We now focus on the cause of bi-stability. Most of the mathematical models for the environmental transmitted diseases exhibit a forward bifurcation at $R_0 = 1$ [52, 38, 6, 11]. In the setting of our work, the bacteria interact with phages; they are no longer free-living. Therefore, it is not surprising for our model to undergo different dynamics. We identified the absorption rate ϵ to be a cause of backward bifurcation, which is precisely the bi-stability phenomenon as articulated in the next proposition.

Proposition 2.6. *In the absence of phage absorption (i.e $\varepsilon = 0$), the model (2.6) undergoes the following dynamics: i) The DFE is globally asymptotically stable whenever $\mathcal{R}_0 \leq 1$. This rules out the possibility of backward bifurcation. ii) If $\mathcal{R}_0 > 1$, there exists a unique endemic equilibrium which is globally asymptotically stable when $\delta = 0$.*

The proof of Proposition 2.6 is given in Appendix E. From the mathematical point of view, the simple and classical threshold dynamics of the model as stated in Proposition 2.6, hinges on the fact that when $\varepsilon = 0$, model (2.6) is dramatically simplified to a model in which the dynamics of phages is decoupled from the rest of the model and the transmission dynamics of cholera follows the mass action principle between humans and bacteria. As from the biologically perspective, the implication of Proposition 2.6 is as follows: in the absence of phage absorption, it is much more easier to eliminate the cholera infection. Indeed it is sufficient to bring the basic reproduction number below the threshold value one.

3. Optimal control

3.1. Controlled model derivation and optimal control problem

In order to reduce the proliferation of bacteria in the environmental reservoir, there are several possible interventions such as disinfection and water sanitation [47], beside the reduction of the number of infected humans using the therapeutic treatments and vaccination strategies [36, 39]. For instance, disinfectants as chemical agents can be designed to inactivate or destroy microorganism such as bacteria. Unfortunately, these chemicals are sometimes toxic to other microorganisms and they usually pollute the environment. On the other hand, the aquatic and soil environments are highly populated by phages, which, unlike chemicals are harmless to soil and water but interact with some bacteria to kill them. Thus using selected virulent phages (specifically, vibriophages) can be an advantage to control the proliferation

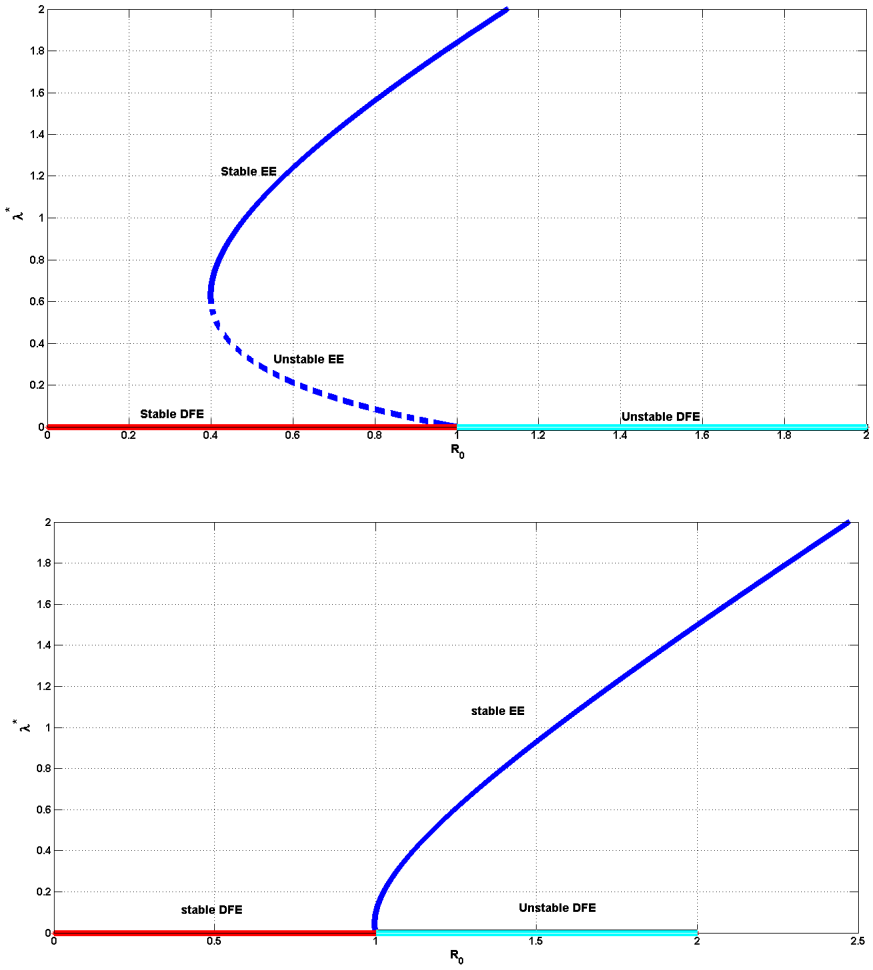

Figure 5: Bifurcation diagrams: Bottom (forward bifurcation in Theorem 2.5) (i). Top (backward bifurcation in Theorem 2.5 (ii)).

of bacteria. In order to control a system of differential equations (*i.e.* to force the solution to follow a specific trajectory), the basic principle of optimal control is often used. The goal is to select a particular control that maximizes or minimizes a chosen objective functional, which is typically a function of some model variables and the control.

To reduce the proportion of lysogen after phage-bacteria interaction, one can increase the number of virulent phages. In this section, we formulate an optimal control model with the release of virulent phages as strategy for cholera elimination. The selection can be done using the techniques in [24, 40]. Indeed, these methods include both desirable characteristics (*i.e.* a relatively broad host range) and a lacking characteristics (*i.e.* carrying toxin genes and the ability to form a lysogen). While phages are first commonly isolated and subsequently characterized, it is possible to alter isolation procedures to bias the isolation toward phages with desirable characteristics. We denote by $h(t)$ the population of virulent phages V shed at time t, μ is the decay rate of V. In our controlled model for cholera, we assume that virulent vibrophages are continuously released into the environment in which vibrio cholerae live and can infect human beings. Denoting by t_f the time at the end of the control, our controlled cholera model

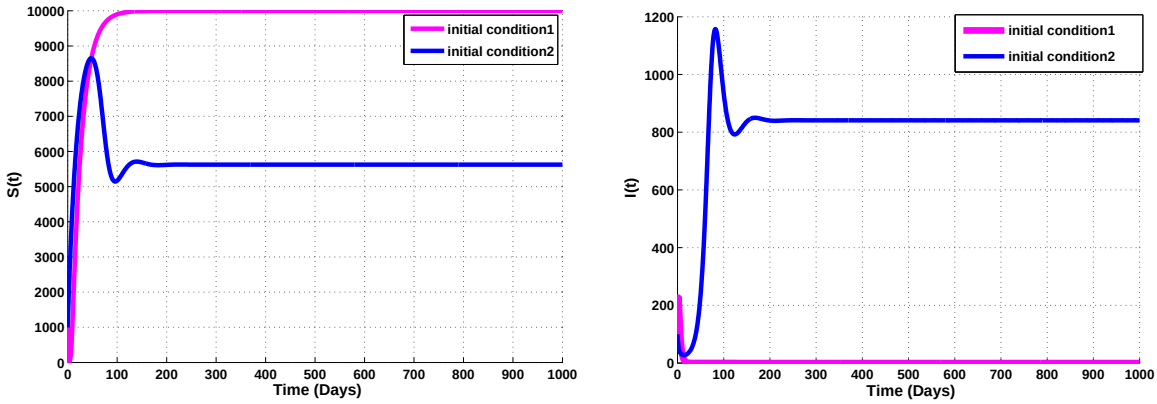

Figure 6: Theorem 2.5 (iii): Bi-stability phenomenon when $\mathcal{R}_0 = 0.1711$. Initial condition 1: $(S_0, I_0, B_0, B_{T0}, B_{V0}, P_0) = (1000, 100, 10^3, 500, 100, 400)$, and initial condition 2: $(S_0, I_0, B_0, B_{T0}, B_{V0}, P_0) = (1000, 100, 10^6, 5 \times 10^4, 100, 400)$

reads as follows:

$$\begin{aligned}
\frac{dS}{dt} &= \Lambda - \beta(B_T + kB)S - \mu_h S + \delta I,\\
\frac{dI}{dt} &= \beta(B_T + kB)S - (\mu_h + d + \delta)I,\\
\frac{dB}{dt} &= \omega I - (\mu_b - r)B - \varepsilon B f(P) - \varepsilon B f(V),\\
\frac{dB_T}{dt} &= \eta I + \phi\pi\varepsilon B f(P) - (\mu_b + \alpha\gamma)B_T, \qquad .\\
\frac{dB_V}{dt} &= \varepsilon B f(V) + \nu I + (1-\pi)\varepsilon B f(P) - (\mu_b + \gamma)B_V,\\
\frac{dP}{dt} &= eI + \theta\gamma B_V + \theta\alpha\gamma B_T - \varepsilon(B_T + B_V + B)P - \mu_P P,\\
\frac{dV}{dt} &= h(t) - \mu V, \quad t \in \left[0, t_f\right].
\end{aligned} \tag{3.1}$$

Model (3.1) is an extension of (2.6) via the inclusion of the continuous release of virulent vibriophages V. This implies the reduction of the population of B by the quantity $\varepsilon B f(V)$ which enters the population of B_V. The objective of the control is to minimize the number of infected individuals (I) and maximize the number of virulent vibriophages at the end of the epidemic period, while keeping the costs of the control as low as possible. To achieve this goal, we incorporate the relative costs associate with each control or combination of policies directed towards controlling the spread of cholera. We define the objective function J and control set Δ as follows:

$$J(h) = \frac{1}{2}\int_0^{t_f} \left(AI + b_1 h^2\right) dt - b_2 V(t_f), \tag{3.2}$$

$$\Delta = \left\{h \in L^1(0, t_f) : h \in [0, h_m], t \in [0, t_f], h_m > 0\right\}.$$

In (3.2), b_1 is the cost of selection and release of virulent phages and b_2 is the cost related to the management of virulent phages V after the selection, A is the social cost which depends on the number

of cholera cases, which in turn are related directly to the number of infected bacteria (B and B_T). Notice that when we minimize the performance index J, the number of virulent phages is maximized.

It is not difficult to prove that there exists an optimal control h^* and a corresponding solution $(S^*, I^*, B^*, B_T^*, B_V^*, P^*, V^*)$ model (3.1) that minimizes the cost function J in Δ [32]:

$$J(h^*) = \min_{h \in \Delta} J(h).$$

The mathematical characterization of the above optimal control for the model (3.1) is stated in the next theorem, whose proof is readily achieved by applying the Pontryagin's Maximum Principle [32].

Theorem 3.1. *Given an optimal control h^* and the corresponding solutions $(S^*, I^*, B^*, B_T^*, B_V^*, P^*, V^*)$, there exist adjoint variables $\lambda_i(t)$ for $i = 1, 2, 3, 4, 5, 6, 7$ satisfying the following system of linear differential equations.*

$$\begin{aligned}
\frac{d\lambda_1}{dt} &= \beta(B_T + kB)(\lambda_1 - \lambda_2) + \lambda_1\mu_h, \\
\frac{d\lambda_2}{dt} &= -A + \delta(\lambda_2 - \lambda_1) + \lambda_2(\mu_h + d) - \lambda_3\omega - \lambda_4\eta - \lambda_5\nu - \lambda_6 e, \\
\frac{d\lambda_3}{dt} &= \beta kS(\lambda_1 - \lambda_2) + \lambda_3(\mu_b - r + \varepsilon f(V) + \varepsilon f(P)) - \varepsilon f(P)(\phi\pi\lambda_4 + (1-\pi)\lambda_5) + \lambda_6\varepsilon P - \varepsilon f(V), \\
\frac{d\lambda_4}{dt} &= \beta S(\lambda_1 - \lambda_2) + \lambda_4(\mu_b + \alpha\gamma) + \lambda_6(\varepsilon P - \theta\alpha\gamma), \\
\frac{d\lambda_5}{dt} &= \lambda_5(\mu_b + \gamma) + \lambda_6(\varepsilon P - \theta\gamma), \\
\frac{d\lambda_6}{dt} &= (\lambda_3 - \phi\pi\lambda_4 - (1-\pi)\lambda_5)\varepsilon B f'(P) + \lambda_6\varepsilon(B + B_T + B_V + \mu_P), \\
\frac{\lambda_7}{dt} &= \lambda_3\varepsilon B f'(V) - \lambda_5\varepsilon B f'(V) - \mu\lambda_7 - b_2,
\end{aligned} \tag{3.3}$$

and the transversality conditions

$$\lambda_i^*(t_f) = 0, \quad i = 1, ..., 7. \tag{3.4}$$

Furthermore,

$$h^* = min\left\{1, max\left(0, \frac{-\lambda_7}{b_1}\right)\right\}. \tag{3.5}$$

3.2. Numerical simulations of the optimal control problem

The simulations are carried out using a set of parameter values giving in Table 1 with $t \in [0, 20]$. We use an iterative scheme to solve the optimality system. We first solve the state equations (3.1) with a guess for the controls over the simulated time using fourth order Runge-Kutta scheme. This is actually the implementation of the so-called "forward-backward sweep method" [32]. Then, we use the current iterative solutions of the state equation to solve the adjoint equations by a backward fourth order Runge-Kutta scheme. The result is displayed on Figures 7 and 8. For the initial condition, $(S_0, I_0, B_0, B_{T0}, B_{V0}, P_0, V_0) = (100, 2, 100, 3, 100, 50, 5)$ and the application of control in 20 days, Figure 7 (left panel) shows that the number of released virulent vibriophages is maximized. This number has increased from 5 to 250 (*i.e.* 4900% increase). The right panel represents the profile of $h(t)$: the release rate of the virulent vibriophages is constant when $t \in [0, 17]$, it decreases exponentially for $t > 17$ to zero at the end of control ($t_f = 20$). On Figure 8, one observes that the control strategy resulted in a significantly

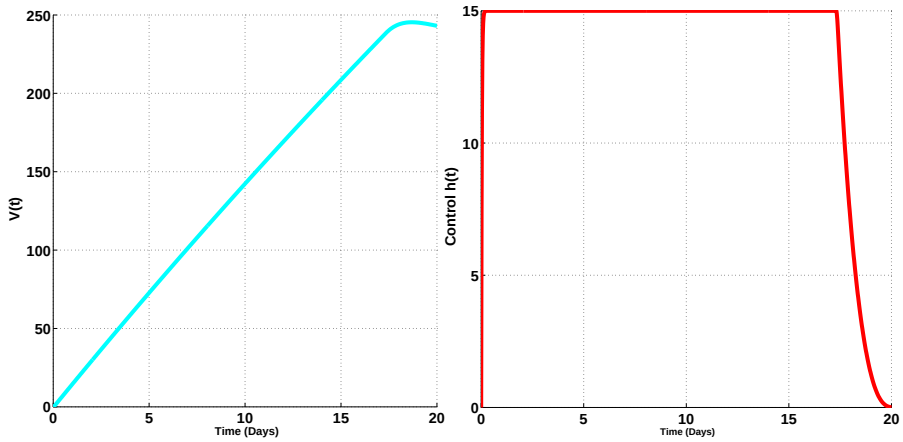

Figure 7: Control function with initial condition $(S_0, I_0, B_0, B_{T0}, B_{V0}, P_0, V_0) = (100, 2, 100, 3, 100, 50, 5)$. The virulent vibriophages V is maximized at the end of control. The profile of $h(t)$ reach the maximum value for $t \in [0, 17]$ and after that $(t > 17)$, it decreases exponentially to zero at the end of control.

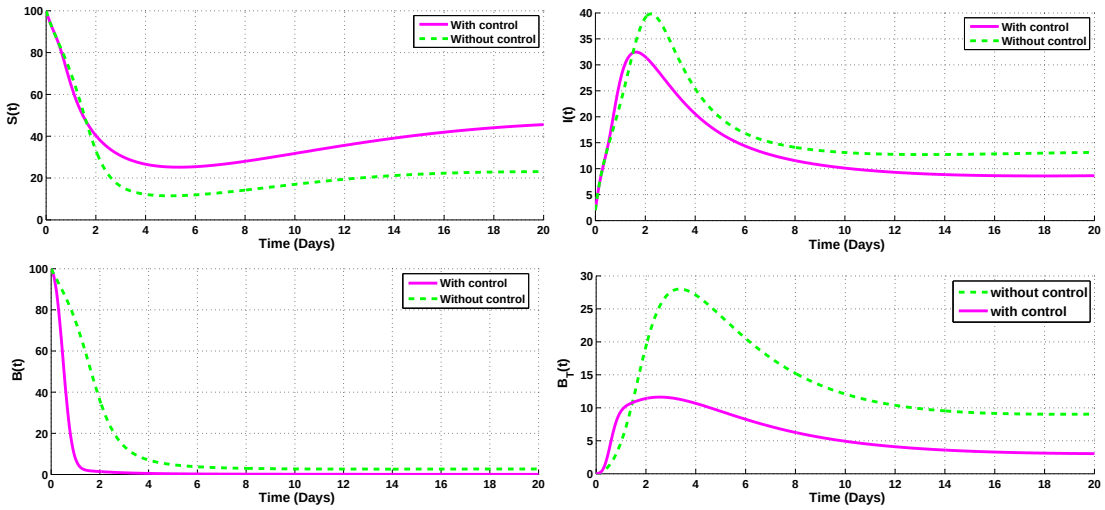

Figure 8: Simulation results of optimal control model (3.1) showing the effect of the released of virulent vibriophages with initial condition $(S_0, I_0, B_0, B_{T0}, B_{V0}, P_0, V_0) = (100, 2, 100, 3, 100, 50, 5)$.

decrease in the number of infected humans (I), susceptible bacteria (B), and lysogen bacteria (B_T) versus a significant increase in the number of susceptible humans (S). Precisely, at the end of the control period of 20 days, our optimal control problem show the reduction of the number infected humans from 15 to 10 cases (*i.e.* 33% decrease). Furthermore, the number of susceptible bacteria vanishes (*i.e.* 100% decrease) and that of lysogen bacteria drops from 9 to 4 (*i.e.*$\approx$ 56% decrease) cells.

4. Conclusion and discussions

The primary goal of this paper is to take the authors' previous works on cholera (*e.g.* [6, 27, 37]) to the next level. That is to add some realism to the control and management of cholera disease through the incorporation of the full life cycle of the phages in their interaction with the vibrio cholerae. This has

been achieved in four directions: (1) mathematical modeling, (2) theoretical, (3) optimal control, and (4) computationally analysis.

(1) From the mathematical modeling perspective, we built a mathematical model describing the impact of phage-bacteria infection on the indirectly transmitted cholera. The novelty includes the use of Smith attachment function as the functional response of the phage-bacteria interaction, the coupling of the predator-prey (phage-bacteria) model with an indirectly transmitted cholera epidemiological model, and the extension of the model by adding a class of virulent vobriophages to control cholera.

(2) From the theoretical point of view, we did an in-depth analysis of the asymptotic behavior of the model without control. We computed the basic reproduction number $\mathcal{R}_0$. Unlike the fact that in the absence of phage absorption, cholera can be eliminated when $\mathcal{R}_0 \leq 1$, we established that the model undergoes the backward bifurcation phenomenon at $\mathcal{R}_0 = 1$ in the presence of phage absorption. We then computed an additional threshold quantity $\mathcal{N}_0$, which led to the following findings: The disease free equilibrium point is globally stable whenever $\mathcal{R}_0 \leq 1$ and $\mathcal{N}_0 \leq 1$. The model without control has multiple endemic equilibrium points depending on the range of $\mathcal{R}_0$ and $\mathcal{N}_0$.

(3) To mitigate the dynamics of cholera, we studied an optimal control problem in which the control strategy consisted in the continuous release of lytic/virulent vibriophages into the contaminated environment. We showed that an optimal control exists and characterized it using the Pontryagin's maximum principle.

(4) Computationally, we used MatLab platform, to perform global sensitivity analysis of the thresholds numbers $\mathcal{R}_0$ and $\mathcal{N}_0$. The result showed that the contact rate β and pathogen decay rate μ_b are the most influential parameters. Thus decreasing β (*i.e.* the improvement of the information about contaminated environment) and increasing μ_b (*i.e.* the use of chemicals to disinfect an environment) might help to reduce $\mathcal{R}_0$ and $\mathcal{N}_0$. Moreover, we simulated the model without control to illustrate our theoretical results. Finally, we solved numerically the optimal control problem by the forward-backward sweep method, to assess the role of using virulent vibriophages on the control of cholera. The numerical result showed that, at the end of control period (20 days), the number of virulent vibriophages is significantly maximized by 4900% and the number of infected humans decreased by 33%. Furthermore, the number of susceptible bacteria vanished (100% reduction) and the number of lysogen bacteria decreased by 56%.

Being an attempt to couple a cholera epidemiological model with an phage-bacteria ecological system, the simple model setting of this work therefore offers many possibilities for extension to increase realism. Firstly, this work can easily be applied to other bacterial-borne infections for which the disease agent interact with a phage specific type in a predator-prey manner. Secondly, following many authors who considered the environment as a reservoir of bacteria (*i.e.* the pathogen growth rate is always greater than its decay rate), we plan to use this assumption to study the existence of periodic solutions of the model without control [37]. This would address the fact that the continuous release of the virulent vibriophages is not that realistic though being mathematically convenient. In practice, releases are rather periodic or instantaneous. To increase realism, impulsive releases are even more convenient because after infection, bacteria need about twenty minutes to burst, which makes it necessary to take a delay into account. All these important features will be incorporated in our future works. Above all, the study of an optimal control problem for a coupled within-host cholera epidemic model and phage-bacteria (predator-prey) interaction model is a path of future investigations [51], including opportunities for phage therapy [49].

Acknowledgments

The second author (BT), acknowledges the support of the University of Pretoria Senior Postdoctoral Program Grant (2018-2020). The authors are grateful to the Editors and the anonymous reviewers whose valuable comments helped to improve the presentation of this manuscript.

Appendixes

Appendix A: Proof of Proposition 2.2

The Jacobian matrix at E_0 is

$$J(E_0) = \begin{pmatrix} -\mu_h & \delta & -\beta k S_0 & -\beta S_0 & 0 & 0 \\ 0 & -(\mu_h + d + \delta) & \beta k S_0 & \beta S_0 & 0 & 0 \\ 0 & \omega & -(\mu_b - r) & 0 & 0 & 0 \\ 0 & \eta & 0 & -(\mu_b + \alpha\gamma) & 0 & 0 \\ 0 & \nu & 0 & 0 & -(\mu_b + \gamma) & 0 \\ 0 & e & 0 & \theta\alpha\gamma & \theta\gamma & -\mu_P \end{pmatrix}.$$

Clearly, $-\mu_h$, $-(\mu_b + \gamma)$ and $-\mu_P$ are eigenvalues of $J(E_0)$. Therefore, the local stability of E_0 is completely determined by the following sub-matrix

$$J_0 = \begin{pmatrix} -(\mu_h + d + \delta) & \beta k S_0 & \beta S_0 \\ \omega & -(\mu_b - r) & 0 \\ \eta & 0 & -(\mu_b + \alpha\gamma) \end{pmatrix}.$$

The characteristic polynomial of J_0 is

$$P(\lambda) = \lambda^3 + a_2\lambda^2 + a_1\lambda + a_0, \tag{4.1}$$

where

$$\begin{cases} a_2 = (\mu_h + d + \delta + \mu_b - r + \mu_b + \alpha\gamma), \\ a_1 = (\mu_h + d + \delta)(\mu_b - r) + (\mu_h + d + \delta)(\mu_b + \alpha\gamma) + (\mu_b + \alpha\gamma)(\mu_b - r) - \beta\omega k S_0 - \beta\eta S_0, \\ a_0 = (\mu_h + d + \delta)(\mu_b - r)(\mu_b + \alpha\gamma)(1 - \mathcal{R}_0). \end{cases} \tag{4.2}$$

It follows from the Routh-Hurwitz criteria [8] that E_0 is locally asymptotically stable if and only if

$$a_2 > 0, a_0 > 0, \quad \text{and} \quad a_1 a_2 > a_0. \tag{4.3}$$

If $\mathcal{R}_0 < 1$, then a_0 is positive and

$$\begin{aligned} a_1 a_2 - a_0 &= a_0 + (\mu_h + d + \delta)^2(\mu_b - r)\left(1 - \frac{\beta k \omega S_0}{(\mu_h + d + \delta)(\mu_b - r)}\right) \\ &+ (\mu_h + d + \delta)^2(\mu_b + \alpha\gamma)\left(1 - \frac{\beta\eta S_0}{(\mu_h + d + \delta)(\mu_b + \alpha\gamma)}\right) \\ &+ (\mu_h + d + \delta)\left[(\mu_b - r)^2 + (\mu_b + \alpha\gamma)^2 + (\mu_b + \alpha\gamma)(\mu_b - r)\right] + (\mu_b + \alpha\gamma)^2(\mu_b - r) \\ &\geq a_0 + (\mu_h + d + \delta)^2\left[(\mu_b - r) + (\mu_b + \alpha\gamma)\right](1 - \mathcal{R}_0) \\ &+ (\mu_h + d + \delta)\left[(\mu_b - r)^2 + (\mu_b + \alpha\gamma)^2 + (\mu_b + \alpha\gamma)(\mu_b - r)\right] + (\mu_b + \alpha\gamma)^2(\mu_b - r) > 0. \end{aligned}$$

Thus the disease free equilibrium point E_0 is locally asymptotically stable whenever $\mathcal{R}_0 < 1$. Conversely, if $R_0 > 1$, then $a_0 < 0$ and E_0 is unstable.

Appendix B: Proof of Theorem 2.3

The proof is done in two steps

Step 1: $\mathcal{N}_0 \leq \mathcal{R}_0 \leq 1$

We consider the following Lyapunov function candidate

$$\mathcal{L} = S - S_0 \ln S + I + \frac{\beta k S_0}{\mu_b - r} B + \frac{\beta S_0}{\mu_b + \alpha\gamma} B_V. \tag{4.4}$$

The derivative of $\mathcal{L}$ alongside the trajectories is

$$\begin{aligned}
\frac{d\mathcal{L}}{dt} &= \left(1 - \frac{S_0}{S}\right)\frac{dS}{dt} + \dot{I} + \frac{\beta k S_0}{\mu_b - r}\frac{dB}{dt} + \frac{\beta S_0}{\mu_b + \alpha\gamma}\frac{dB_V}{dt} \\
&= \left(1 - \frac{S_0}{S}\right)(\Lambda - \beta B_T S - \beta k B S - \mu_h S + \delta I) + (\beta B_T S + \beta k B S - (\mu_h + d + \delta) I) \\
&+ \frac{\beta k S_0}{\mu_b - r}(\omega I - (\mu_b - r) B - \varepsilon B f(P)) + \frac{\beta S_0}{\mu_b + \alpha\gamma}(\eta I + \phi\pi\varepsilon B f(P) - (\mu_b + \alpha\gamma) B_T).
\end{aligned}$$

After some computation

$$\begin{aligned}
\frac{d\mathcal{L}}{dt} &= -\frac{\mu_h}{S}(S - S_0)^2 + \beta B_T S_0 + \beta k B S_0 - (\mu_h + d + \delta) I + \frac{\beta\omega K S_0}{\mu_b - r} I - \beta k S_0 B - \frac{\beta k S_0}{\mu_b - r}\varepsilon B f(P) \\
&+ \frac{\beta\eta S_0}{\mu_b + \alpha\gamma} I + \frac{\beta S_0}{\mu_b + \alpha\gamma}\phi\pi\varepsilon B f(P) - \beta S_0 B_T \\
&= -\frac{\mu_h}{S}(S - S_0)^2 + I\left(\frac{\beta\omega K S_0}{\mu_b - r} + \frac{\beta\eta S_0}{\mu_b + \alpha\gamma} - (\mu_h + d + \delta)\right) + \varepsilon B f(P)\left(\frac{\beta\phi\pi S_0}{\mu_b + \alpha\gamma} - \frac{\beta k S_0}{\mu_b - r}\right).
\end{aligned}$$

Knowing that

$$\frac{\beta\phi\pi S_0}{\mu_b + \alpha\gamma} - \frac{\beta k S_0}{\mu_b - r} = (\mathcal{N}_0 - \mathcal{R}_0)\frac{\mu_h + d + \delta}{\omega},$$

we have

$$\begin{aligned}
\frac{d\mathcal{L}}{dt} &= -\frac{\mu_h}{S}(S - S_0)^2 + I(\mu_h + d + \delta)\left(\frac{\beta\omega k S_0}{(\mu_b - r)(\mu_h + d + \delta)} + \frac{\beta\eta S_0}{(\mu_b + \alpha\gamma)(\mu_h + d + \delta)} - 1\right) \\
&+ \varepsilon B f(P)\left(\frac{\beta\phi\pi S_0}{\mu_b + \alpha\gamma} - \frac{\beta k S_0}{\mu_b - r}\right) \\
&= -\frac{\mu_h}{S}(S - S_0)^2 + I(\mu_h + d + \delta)(\mathcal{R}_0 - 1) + \varepsilon B f(P)(\mathcal{N}_0 - \mathcal{R}_0).
\end{aligned}$$

Since $\mathcal{N}_0 \leq \mathcal{R}_0 \leq 1$, $d\mathcal{L}/dt \leq 0$ and $\mathcal{L}$ is indeed a Lyapunov function. Moreover, the largest invariant set contained in Ω such that $d\mathcal{L}/dt = 0$ is $\{E_0\}$. The application of LaSalle's Invariance Principle [19] proves that the DFE is globally asymptotically stable in Ω.

Step 2: $\mathcal{R}_0 \leq \mathcal{N}_0 \leq 1$

We consider the following Lyapunov function candidate

$$\mathcal{L} = S - S_0 \ln S + I + \frac{\phi\pi(\mu_h + d + \delta)}{\omega\phi\pi + \eta} B + \frac{(\mu_h + d + \delta)}{\omega\phi\pi + \eta} B_V. \tag{4.5}$$

One has

$$\begin{aligned}
\frac{d\mathcal{L}}{dt} &= \left(1-\frac{S_0}{S}\right)\frac{dS}{dt}+\frac{dI}{dt}+\frac{\phi\pi(\mu_h+d+\delta)}{\omega\phi\pi+\eta}\frac{dB}{dt}+\frac{(\mu_h+d+\delta)}{\omega\phi\pi+\eta}\frac{dB_V}{dt}\\
&= \left(1-\frac{S_0}{S}\right)(\Lambda-\beta B_T S-\beta kBS-\mu_h S+\delta I)+(\beta B_T S+\beta kBS-(\mu_h+d+\delta)I)\\
&+ \frac{\phi\pi(\mu_h+d+\delta)}{\omega\phi\pi+\eta}(\omega I-(\mu_b-r)B-\varepsilon Bf(P))+\frac{(\mu_h+d+\delta)}{\omega\phi\pi+\eta}(\eta I+\pi\varepsilon Bf(P)-(\mu_b+\alpha\gamma)B_T)\\
&= -\frac{\mu_h}{S}(S-S_0)^2+B\left(\beta kS_0-\frac{\phi\pi(\mu_b-r)(\mu_h+d+\delta)}{\omega\phi\pi+\eta}\right)+B_T\left(\beta S_0-\frac{(\mu_b+\alpha\gamma)(\mu_h+d+\delta)}{\omega\phi\pi+\eta}\right)\\
&= -\frac{\mu_h}{S}(S-S_0)^2+\frac{(\mu_b-r)\phi\pi(\mu_h+d+\delta)}{\phi\pi\omega+\eta}B\left(\frac{\beta k\omega S_0}{(\mu_b-r)(\mu_h+d+\delta)}+\frac{\beta\eta kS_0}{\phi\pi(\mu_b-r)(\mu_h+d+\delta)}-1\right)\\
&+ \frac{(\mu_b+\alpha\gamma)(\mu_h+d+\delta)}{\phi\pi\omega+\eta}B_T\left(\frac{\beta\omega\phi\pi S_0}{(\mu_b+\alpha\gamma)(\mu_h+d+\delta)}+\frac{\beta\eta S_0}{(\mu_b+\alpha\gamma)(\mu_h+d+\delta)}-1\right)
\end{aligned}$$

$\mathcal{R}_0\le\mathcal{N}_0\le 1$ implies that $\dfrac{k}{\phi\pi(\mu_b-r)}\le\dfrac{1}{\mu_b+\alpha\gamma}$, hence

$$\begin{aligned}
\frac{d\mathcal{L}}{dt} &\le -\frac{\mu_h}{S}(S-S_0)^2+\frac{(\mu_b-r)\phi\pi(\mu_h+d+\delta)}{\phi\pi\omega+\eta}B\left(\frac{\beta k\omega S_0}{(\mu_b-r)(\mu_h+d+\delta)}+\frac{\beta\eta S_0}{(\mu_b+\alpha\gamma)(\mu_h+d+\delta)}-1\right)\\
&+ \frac{(\mu_b+\alpha\gamma)(\mu_h+d+\delta)}{\phi\pi\omega+\eta}B_T\left(\frac{\beta\omega\phi\pi S_0}{(\mu_b+\alpha\gamma)(\mu_h+d+\delta)}+\frac{\beta\eta S_0}{(\mu_b+\alpha\gamma)(\mu_h+d+\delta)}-1\right)\\
&= -\frac{\mu_h}{S}(S-S_0)^2+\frac{(\mu_b-r)\phi\pi(\mu_h+d+\delta)}{\phi\pi\omega+\eta}B\left(\mathcal{R}_0-1\right)+\frac{(\mu_b+\alpha\gamma)(\mu_h+d+\delta)}{\phi\pi\omega+\eta}B_T\left(\mathcal{N}_0-1\right).
\end{aligned}$$

Since $\mathcal{R}_0\le\mathcal{N}_0\le 1$, $d\mathcal{L}/dt\le 0$ and $\mathcal{L}$ is indeed a Lyapunov function. Moreover, the largest invariant set contained in Ω such that $d\mathcal{L}/dt=0$ is $\{E_0\}$. LaSalle's Invariance Principle [19] permits to conclude that the DFE is globally asymptotically stable in Ω.
Combining the conclusions of step 1 and step 2, the DFE is globally asymptotically stable.

Appendix C: Proof of Theorem 2.4

Set $E^*=(S^*,I^*,B^*,B_T^*,B_V^*,P^*)$ any endemic equilibrium of the model (2.6). At E^* one has

$$\begin{cases}
\Lambda-\beta(B_T^*+kB^*)S^*-\mu_h S^*+\delta I^*=0,\\
\beta(B_T^*+kB^*)S^*-(\mu_h+d+\delta)I^*=0,\\
\omega I^*-(\mu_b-r)B^*-\varepsilon B^* f(P^*)=0,\\
\eta I^*+\phi\pi\varepsilon B^* f(P^*)-(\mu_b+\alpha\gamma)B_T^*=0,\\
\nu I^*+(1-\pi)\varepsilon B^* f(P^*)-(\mu_b+\gamma)B_V^*=0,\\
eI^*+\theta\alpha B_V^*+\theta\alpha\gamma B_T^*-\varepsilon(B_T^*+B_V^*+B^*)P^*-\mu_P P^*=0.
\end{cases}\tag{4.6}$$

Set $\lambda^*=\beta(B_T^*+kB^*)$, from the the second equation of (4.6)

$$I^*=\frac{\lambda^* S^*}{\mu_h+d+\delta}.\tag{4.7}$$

Putting (4.7) in the first equation of (4.6) yields

$$S^* = \frac{\Lambda(\mu_h + d + \delta)}{\lambda^*(\mu_h + d) + \mu_h(\mu_h + d + \delta)}. \tag{4.8}$$

Replacing in (4.7), we have the following form

$$I^* = \frac{\Lambda\lambda^*}{\lambda^*(\mu_h + d) + \mu_h(\mu_h + d + \delta)}. \tag{4.9}$$

From the third equation of (4.6),

$$B^* = \frac{\omega I^*}{\mu_b - r + \varepsilon f(P^*)}$$

and using (4.9) yields

$$B^* = \frac{\omega\Lambda\lambda^*}{(\mu_b - r + \varepsilon f(P^*))\,(\lambda^*(\mu_h + d) + \mu_h(\mu_h + d + \delta))}. \tag{4.10}$$

By the same way, from the fourth equation of (2.4),

$$B_T^* = \frac{\left[\varepsilon f(P^*)(\eta + \phi\pi\omega) + \eta(\mu_b - r)\right]\Lambda\lambda^*}{(\mu_b + \alpha\gamma)(\mu_b - r + \varepsilon f(P^*))(\lambda^*(\mu_h + d) + \mu_h(\mu_h + d + \delta))}. \tag{4.11}$$

Now use the notation of λ^*, one has the following

$$\begin{aligned} \lambda^* &= \beta(B_T^* + kB^*) \\ &= \frac{\left[\beta k\omega(\mu_b + \alpha\gamma) + \beta\varepsilon f(P^*)(\eta + \phi\pi\omega) + \beta\eta(\mu_b - r)\right]\Lambda\lambda^*}{(\mu_b + \alpha\gamma)(\mu_b - r + \varepsilon f(P^*))(\lambda^*(\mu_h + d) + \mu_h(\mu_h + d + \delta))}. \end{aligned}$$

Since we are interested in the positive values of λ^*, after some computations we have the following form

$$\lambda^* = \frac{\mu_h(\mu_h + d + \delta)\left[(\mu_b - r)(\mathcal{R}_0 - 1) + \varepsilon f(P^*)(\mathcal{N}_0 - 1)\right]}{(\mu_b - r)(\mu_h + d) + (\mu_h + d)\varepsilon f(P^*)}. \tag{4.12}$$

Using (4.12) in (4.10) and (4.11), B^* and B_T^* become

$$B^* = \frac{\omega\Lambda\left[(\mu_b - r)(\mathcal{R}_0 - 1) + \varepsilon f(P^*)(\mathcal{N}_0 - 1)\right]}{(\mu_h + d)(\mu_b - r + \varepsilon f(P^*))\left[(\mu_b - r)\mathcal{R}_0 + \varepsilon f(P^*)\mathcal{N}_0\right]} \tag{4.13}$$

and,

$$B_T^* = \frac{\Lambda\left[\eta(\mu_b - r) + (\eta + \pi\omega)\varepsilon f(P^*)\right]\left[(\mu_b - r)(\mathcal{R}_0 - 1) + \varepsilon f(P^*)(\mathcal{N}_0 - 1)\right]}{(\mu_b + \alpha\gamma)(\mu_h + d)(\mu_b - r + \varepsilon f(P^*))\left[(\mu_b - r)\mathcal{R}_0 + \varepsilon f(P^*)\mathcal{N}_0\right]}. \tag{4.14}$$

On the other hand, the fifth and sixth equations of (4.6) yield,

$$B_V^* = \frac{\Lambda\left[\nu(\mu_b - r) + (\nu + (1 - \pi)\omega)\varepsilon f(P^*)\right]\left[(\mu_b - r)(\mathcal{R}_0 - 1) + \varepsilon f(P^*)(\mathcal{N}_0 - 1)\right]}{(\mu_b + \gamma)(\mu_h + d)(\mu_b - r + \varepsilon f(P^*))\left[(\mu_b - r)\mathcal{R}_0 + \varepsilon f(P^*)\mathcal{N}_0\right]} \tag{4.15}$$

and

$$P^* = \frac{\theta\alpha\gamma B_T^* + \theta\gamma B_V^* + eI^*}{\varepsilon(B^* + B_T^* + B_V^*) + \mu_P}. \tag{4.16}$$

Plugging the expressions of B^*, B_T^* and B_V^* into (4.16) yields

$$\Psi(P^*) = \Phi(P^*), \tag{4.17}$$

where

$$\begin{aligned}\Psi(P^*) &= P^*\Big[\varepsilon\Lambda\omega(\mu_b+\alpha\gamma)(\mu_b+\gamma)+\varepsilon\Lambda(\mu_b-r)[(\mu_b+\gamma)\eta+(\mu_b+\alpha\gamma)\nu]\\ &+ e\mu_P(\mu_b+\alpha\gamma)(\mu_b+\gamma)(\mu_b-r)^2\mathcal{R}_0+[\varepsilon\Lambda(\mu_b+\gamma(\eta+\phi\pi\omega)+\varepsilon\Lambda(\mu_b+\alpha\gamma)(\nu+(1-\pi)\omega)\\ &+ e\mu_P(\mu_b+\gamma)(\mu_b+\alpha\gamma)(\mu_b-r)(\mathcal{R}_0+\mathcal{N}_0)]\varepsilon f(P^*)+e\mu_P(\mu_b+\alpha\gamma)\mathcal{N}_0\varepsilon^2 f^2(P^*)\Big]\end{aligned}$$

and

$$\begin{aligned}\Phi(P^*) &= \theta\gamma\Lambda\Big[(\mu_b+\gamma)\alpha(\omega\phi\pi+\eta)+(\mu_b+\alpha\gamma)(\nu+(1-\pi)\omega)\Big](\mathcal{N}_0-1)\varepsilon f^2(P^*)\\ &+ \theta\gamma(\mu_b-r)\Lambda\Big[(\eta(\mu_b+\gamma)+\nu(\mu_b+\alpha\gamma)\Big]\varepsilon f(P^*)(\mathcal{N}_0-1)\\ &+ \theta\gamma(\mu_b-r)\Big[(\mu_b+\gamma)\alpha(\eta+\phi\pi\omega)+(\mu_b+\alpha\gamma)(\nu+(1-\pi)\omega)\Big]\varepsilon f(P^*)(\mathcal{R}_0-1)\\ &+ \theta\gamma(\mu_b-r)^2\Lambda(\eta(\mu_b+\gamma)+\nu(\mu_b+\alpha\gamma))(\mathcal{R}_0-1).\end{aligned}$$

The straightforward calculations give

$$\Psi(0)=0,\quad \text{and}\quad \Phi(0)=\theta\gamma(\mu_b-r)^2\Lambda\left[\eta(\mu_b+\gamma)+\nu(\mu_b+\alpha\gamma)\right](\mathcal{R}_0-1).$$

$$\begin{aligned}\Psi'(P^*) &= \varepsilon\Lambda\omega(\mu_b+\alpha\gamma)(\mu_b+\gamma)+\varepsilon\Lambda(\mu_b-r)[(\mu_b+\gamma)\eta+(\mu_b+\alpha\gamma)\nu]\\ &+ \mu_P(\mu_b+\alpha\gamma)(\mu_b+\gamma)(\mu_b-r)^2\mathcal{R}_0+[\varepsilon\Lambda(\mu_b+\gamma(\eta+\phi\pi\omega)+\varepsilon\Lambda(\mu_b+\alpha\gamma)(\nu+(1-\pi)\omega)\\ &+ e\mu_P(\mu_b+\gamma)(\mu_b+\alpha\gamma)(\mu_b-r)(\mathcal{R}_0+\mathcal{N}_0)]\varepsilon f(P^*)+\mu_P(\mu_b+\alpha\gamma)\mathcal{N}_0\varepsilon^2 f^2(P^*)\\ &+ P^*\Big[\varepsilon\Lambda\omega(\mu_b+\alpha\gamma)(\mu_b+\gamma)+\varepsilon\Lambda(\mu_b-r)[(\mu_b+\gamma)\eta+(\mu_b+\alpha\gamma)\nu]\\ &+ \mu_P(\mu_b+\alpha\gamma)(\mu_b+\gamma)(\mu_b-r)^2\mathcal{R}_0+[\varepsilon\Lambda(\mu_b+\gamma(\eta+\phi\pi\omega)+\varepsilon\Lambda(\mu_b+\alpha\gamma)(\nu+(1-\pi)\omega)\\ &+ e\mu_P(\mu_b+\gamma)(\mu_b+\alpha\gamma)(\mu_b-r)(\mathcal{R}_0+\mathcal{N}_0)]\varepsilon f'(P^*)+e\mu_P(\mu_b+\alpha\gamma)\mathcal{N}_0\varepsilon^2 2f'(P^*)f(P^*)\Big]\end{aligned}$$

and

$$\begin{aligned}\Phi'(P^*) &= 2\theta\gamma\Lambda\Big[(\mu_b+\gamma)\alpha(\omega\phi\pi+\eta)+(\mu_b+\alpha\gamma)(\nu+(1-\pi)\omega)\Big](\mathcal{N}_0-1)\varepsilon f'(P^*)f(P^*)\\ &+ \theta\gamma(\mu_b-r)\Lambda\Big[(\eta(\mu_b+\gamma)+\nu(\mu_b+\alpha\gamma)\Big]\varepsilon f'(P^*)(\mathcal{N}_0-1)\\ &+ \theta\gamma(\mu_b-r)\Big[(\mu_b+\gamma)\alpha(\eta+\phi\pi\omega)+(\mu_b+\alpha\gamma)(\nu+(1-\pi)\omega)\Big]\varepsilon f'(P^*)(\mathcal{R}_0-1).\end{aligned}$$

Recalling that, the Smith attachment function $f(P)$ satisfies $f'(P)>0$ and $\lim_{P\to+\infty} f(P)=n$, we conclude that $\Psi'(P)>0$, $\lim_{P^*\to+\infty}\Psi(P^*)=+\infty$ and $\lim_{P^*\to+\infty}\Phi(P^*)=y_0$ with

$$\begin{aligned}y_0 &= \theta\gamma\Lambda\left\{(\mu_b+\gamma)\alpha(\omega\phi\pi+\eta)+(\mu_b+\alpha\gamma)(\nu+(1-\pi)\omega)\Big)\varepsilon n^2+(\mu_b-r)\Big((\eta(\mu_b+\gamma)+\nu(\mu_b+\alpha\gamma)\Big)\varepsilon n\right\}(\mathcal{N}_0-1)\\ &+\left\{(\mu_b-r)\Big((\mu_b+\gamma)\alpha(\eta+\phi\pi\omega)+(\mu_b+\alpha\gamma)(\nu+(1-\pi)\omega)\Big)\varepsilon n+(\mu_b-r)^2(\eta(\mu_b+\gamma)+\nu(\mu_b+\alpha\gamma))\right\}(\mathcal{R}_0-1).\end{aligned}$$

Thus, Ψ is an increasing function and Φ has an horizontal asymptote $y=y_0$. Note that the sign of y_0 depends on the values of $\mathcal{R}_0$ and $\mathcal{N}_0$.

The existence and the number of positive endemic equilibrium points of (2.6) depends on the intersection points of the graphs of Ψ and Φ. We proceed by inspection to investigate the number of the positive roots of equation (4.17).

i) $\mathcal{R}_0\le 1$, and $\mathcal{N}_0\le 1$. In this case Φ is decreasing function and $\Phi(0)\le 0$. Since Ψ is increasing and $\Psi(0)=0$. The graphs of Ψ and Φ do not intersect.

ii) $\mathcal{R}_0>1$, and $\mathcal{N}_0>1$. In this case Φ is increasing, $\Phi(0)>0$ and $y_0>0$. Since Ψ is increasing and $\Psi(0)=0$ there is only one intersection point of graphs of Ψ and Φ.

iii) Otherwise, there is one or at least three intersections points between Ψ and Φ.

Appendix D: Proof of Theorem 2.5

To explore the possibility of a backward bifurcation in the model (2.6), we introduce the following notations, we re-label the variables $S = x_1, I = x_2, B = x_3, B_T = x_4, B_V = x_5, P = x_6$. Further, by introducing the vector notation $X = (x_1, x_2, x_3, x_4, x_5, x_6)^T$ (2.6) has the form $\frac{dX}{dt} = F(X)$, where $F = (f_1, f_2, f_3, f_4, f_5, f_6)$, as follows:

$$\begin{cases} \frac{dx_1}{dt} = f_1 = \Lambda - \beta(x_4 + kx_3)x_1 - \mu_h x_1 + \delta x_2, \\ \frac{dx_2}{dt} = f_2 = \beta(x_4 + kx_3)x_1 - (\mu_h + d + \delta)x_2, \\ \frac{dx_3}{dt} = f_4 = \omega x_2 - (\mu_b - r)x_3 - \varepsilon x_3 f(x_6), \\ \frac{dx_4}{dt} = f_5 = \eta x_2 + \phi\pi\varepsilon x_3 f(x_6) - (\mu_b + \alpha\gamma)x_4, \\ \frac{dx_5}{dt} = f_6 = \nu x_2 + (1-\pi)\varepsilon x_3 f(x_6) - (\mu_b + \gamma)x_6, \\ \frac{dx_6}{dt} = f_7 = e x_2 + \theta\alpha x_5 + \theta\alpha\gamma x_4 - \varepsilon(x_3 + x_4 + x_5)x_6 - \mu_P x_6. \end{cases} \tag{4.18}$$

Theorem 4.1 in [10] will be used to determined whether or not the model (2.6) exhibits a backward bifurcation at $\mathcal{R}_0 = 1$. We set β as the bifurcation parameter. Solving for β the equation $\mathcal{R}_0 = 1$ gives $\beta = \beta^*$. The jacobian matrix of (4.21) is

$$J^* = \begin{pmatrix} -\mu_h & \delta & -\beta^* k S_0 & -\beta^* S_0 & 0 & 0 \\ 0 & -(\mu_h + d + \delta) & \beta^* k S_0 & \beta^* S_0 & 0 & 0 \\ 0 & \omega & -(\mu_b - r) & 0 & 0 & 0 \\ 0 & \eta & 0 & -(\mu_b + \alpha\gamma) & 0 & 0 \\ 0 & \nu & 0 & 0 & -(\mu_b + \gamma) & 0 \\ 0 & e & 0 & \theta\alpha\gamma & \theta\gamma & -\mu_P \end{pmatrix}.$$

After some computations, the right eigenvector of J^* is $w = (w_1, w_2, w_3, w_4, w_5, w_6)^T$, where,

$$w_1 = -\frac{(\mu_h + d)}{\mu_h},\ w_2 = 1,\ w_3 = \frac{\omega}{\mu_b - r},\ w_4 = \frac{\eta}{\mu_b + \alpha\gamma},\ w_5 = \frac{\nu}{\mu_b + \gamma}$$

and

$$w_6 = \frac{\theta\alpha\gamma\eta}{\mu_P(\mu_b + \alpha\gamma)} + \frac{\theta\gamma\nu}{\mu_P(\mu_b + \gamma)} + \frac{e}{\mu_P(\mu_h + d + \delta)}.$$

The left eigenvector associated to J^* is given by $v = (v_1, v_2, v_3, v_4, v_5, v_6)$ where,

$$v_1 = 0,\ v_2 = 1,\ v_3 = \frac{\beta^* k}{\mu_b - r},\ v_4 = \frac{\beta^*}{\mu_b + \alpha\gamma},\ v_5 = 0,\ v_6 = 0.$$

Now using the equality

$$\frac{df}{dP}(0) = \frac{F_n(0)}{(F_n(0))^2} = 1,$$

The nonzero second partial derivatives of F are:

$$\frac{\partial^2 f_2}{\partial x_1 \partial x_3} = \frac{\partial^2 f_2}{\partial x_3 \partial x_1} = \beta k,\ \frac{\partial^2 f_2}{\partial x_1 \partial x_4} = \frac{\partial^2 f_2}{\partial x_4 \partial x_1} = \beta,\ \frac{\partial^2 f_3}{\partial x_3 \partial x_6} = \frac{\partial^2 f_3}{\partial x_6 \partial x_3} = \varepsilon,$$

$$\frac{\partial^2 f_4}{\partial x_3 \partial x_6} = \frac{\partial^2 f_4}{\partial x_6 \partial x_3} = \phi\pi\varepsilon\frac{\partial^2 f_2}{\partial x_3 \partial \beta^*} = \beta S_0,\ \frac{\partial^2 f_2}{\partial x_4 \partial \beta^*} = S_0.$$

Thus, we define and compute the numbers $\mathcal{A}$ and $\mathcal{B}$ as follows:

$$\begin{aligned}
\mathcal{A} &= v_2 \sum_{i,j=1}^{6} w_i w_j \frac{\partial^2 f_2}{\partial x_i \partial x_j}(0,0) + v_3 \sum_{i,j=1}^{6} w_i w_j \frac{\partial^2 f_3}{\partial x_i \partial x_j}(0,0) + v_4 \sum_{i,j=1}^{6} w_i w_j \frac{\partial^2 f_4}{\partial x_i \partial x_j}(0,0) \\
&= 2\left[w_1(\beta^* k w_3 + \beta^* w_4) + \frac{\varepsilon w_6}{S_0 \omega}\left(\frac{\beta^* \phi \pi \omega S_0}{\mu_b + \alpha\gamma} - \frac{\beta^* \omega S_0}{\mu_b - r}\right)\right] \\
&= -2\frac{\mu_h + d}{\mu_h}\left(\frac{\beta^* k \omega}{\mu_b - r} + \frac{\beta^* \eta}{\mu_b + \alpha\gamma}\right) \\
&+ 2\frac{\varepsilon}{S_0(\mu_b - r)}\left(\frac{\theta\alpha\gamma\eta}{\mu_P(\mu_b + \alpha\gamma)} + \frac{\theta\gamma\nu}{\mu_P(\mu_b + \gamma)} + \frac{e}{\mu_P(\mu_h + d + \delta)}\right)\left(\frac{\beta^* \phi \pi \omega S_0}{\mu_b + \alpha\gamma} - \frac{\beta^* \omega S_0}{\mu_b - r}\right).
\end{aligned}$$

We note that

$$\begin{aligned}
\left(\frac{\beta^* \phi \pi \omega S_0}{\mu_b + \alpha\gamma} - \frac{\beta^* \omega S_0}{\mu_b - r}\right) &= \left(\frac{\beta^* \phi \pi \omega S_0}{\mu_b + \alpha\gamma} + \frac{\beta^* \eta S_0}{\mu_b + \alpha\gamma} - \frac{\beta^* \eta S_0}{\mu_b + \alpha\gamma} - \frac{\beta^* \omega S_0}{\mu_b - r}\right) \\
&= (\mu_h + d + \delta)(\mathcal{N}_0 - \mathcal{R}_0) \quad \text{with} \quad \mathcal{R}_0 = 1 \\
&= (\mu_h + d + \delta)(\mathcal{N}_0 - 1).
\end{aligned}$$

Finally $\mathcal{A}$ can be rewritten in the following form

$$\mathcal{A} = 2\frac{\varepsilon(\mu_h + d + \delta)}{S_0(\mu_b - r)}\left(\frac{\theta\alpha\gamma\eta}{\mu_P(\mu_b + \alpha\gamma)} + \frac{\theta\gamma\nu}{\mu_P(\mu_b + \gamma)} + \frac{e}{\mu_P(\mu_h + d + \delta)}\right)(\mathcal{N}_0 - \chi_0). \tag{4.19}$$

and

$$\mathcal{B} = \sum_{k,i=1}^{6} v_k w_i \frac{\partial^2 f_k}{\partial x_i \partial \tau}(0,0) = \left(\frac{\omega k}{\mu_b - r} + \frac{\eta}{\mu_b + \alpha\gamma}\right) S_0 > 0.$$

From (4.19) one can easily make the following conclusion

i. If $\mathcal{N}_0 < \chi_0$, (or equivalently $\mathcal{A} < 0$), then according to Theorem 4.1 in [10], model (2.6) exhibits a forward bifurcation.

ii. If $\mathcal{N}_0 > \chi_0$ (or equivalently $\mathcal{A} > 0$), then thanks to Theorem 4.1 in [10], model (2.6) exhibits a bi-stability through a backward bifurcation phenomenon.

This completes the proof.

Appendix E: Proof of Proposition 2.6

i) We consider the following Lyapunov function

$$\mathcal{L}_0 = S - S_0 \ln S + I + \frac{\beta k S_0}{\mu_b - r} B + \frac{\beta S_0}{\mu_b + \alpha\gamma} B_V. \tag{4.20}$$

From the proof of Theorem 2.3 one has

$$\frac{d\mathcal{L}_0}{dt} = -\frac{\mu_h}{S}(S - S_0)^2 + I(\mu_h + d + \delta)(\mathcal{R}_0 - 1) \leq 0.$$

Moreover, the largest invariant set such that $d\mathcal{L}_0/dt = 0$ is the DFE $(S_0, 0, 0, 0, 0, 0)$. Thus, by the classical Lyapunov theorem and the LaSalle's Invariance Principle, the global stability of the disease-free equilibrium E_0 is guaranteed. ii) From the proof of the Theorem 2.4 one easily have

$$\begin{cases} S^* = \dfrac{\Lambda(\mu_h + d + \delta)(\mu_b - r)(\mu_b + \alpha\gamma)}{\beta(\mu_h + d)\left(\eta\Lambda(\mu_b - r) + k\omega(\mu_b + \alpha\gamma)\right)(\mathcal{R}_0 - 1) + (\mu_b + \alpha\gamma)(\mu_b - r)\mu_h(\mu_h + d + \delta)}, \\ I^* = \dfrac{\beta\Lambda^2\left(\eta\Lambda(\mu_b - r) + k\omega(\mu_b + \alpha\gamma)\right)(\mathcal{R}_0 - 1)}{\beta(\mu_h + d)\left(\eta\Lambda(\mu_b - r) + k\omega(\mu_b + \alpha\gamma)\right)(\mathcal{R}_0 - 1) + (\mu_b + \alpha\gamma)(\mu_b - r)\mu_h(\mu_h + d + \delta)}, \\ B^* = \dfrac{\omega\Lambda\left(\mathcal{R}_0 - 1\right)}{(\mu_h + d)(\mu_b - r)\mathcal{R}_0}, \\ B_T^* = \dfrac{\eta\Lambda\left(\mathcal{R}_0 - 1\right)}{(\mu_h + d)(\mu_b + \alpha\gamma)\mathcal{R}_0}, \\ B_V^* = \dfrac{\nu\Lambda\left(\mathcal{R}_0 - 1\right)}{(\mu_h + d)(\mu_b + \gamma)\mathcal{R}_0}, \\ P^* = \dfrac{\Lambda\left(\theta\alpha\gamma\eta(\mu_b + \gamma) + \theta\gamma\nu(\mu_b + \alpha\gamma)\right)(\mathcal{R}_0 - 1)}{\left(\eta(\mu_b - r)(\mu_b + \gamma) + \nu(\mu_b - r)(\mu_b + \alpha\gamma)\right)(\mathcal{R}_0 - 1) + \mu_P(\mu_b - r)(\mu_h + d)(\mu_b + \alpha\gamma)(\mu_b + \gamma)}. \end{cases} \tag{4.21}$$

For the global stability of the endemic equilibrium point, we consider the following Lyapunov function

$$\mathcal{L}_1 = S - S^* \ln S + I - I^* \ln I + \frac{\beta k S^* B^*}{\omega I^*}\left(B - B^* \ln B\right) + \frac{\beta S^* B_T^*}{\eta I^*}\left(B_T - B_T^* \ln B_T\right). \tag{4.22}$$

The straightforward computation of the derivative of $\mathcal{L}_1$ alongside the trajectories of (2.6) is

$$\frac{d\mathcal{L}_1}{dt} = -\mu_h\frac{(S - S^*)^2}{S} + \beta S^* B_T^*\left(3 - \frac{S^*}{S} - \frac{B_T^* I}{B_T I^*} - \frac{B_T S I^*}{B_T^* S^* I}\right) + \beta k S^* B^*\left(3 - \frac{S^*}{S} - \frac{B^* I}{B I^*} - \frac{B S I^*}{B^* S^* I}\right) \leq 0. \tag{4.23}$$

Finally, using the arithmetic-geometric means inequality, $n - (y_1 + y_2 + ... + y_n) \leq 0$, where $y_1 y_2 ... y_n = 1$, and y_1 , y_2 , $...y_n > 0$, it follows that $d\mathcal{L}_1/dt \leq 0$. Furthermore, the largest invariant such that $d\mathcal{L}_1/dt = 0$ is the singleton $\{(S^*, I^*, B^*, B_T^*, B_V^*, P^*)\}$. The global stability of the endemic equilibrium point E^* follows from the classical stability theorem of Lyapunov and LaSalle's Invariance Principle.

References

[1] H. Abboubakar, J.C. Kamgang, D. Tieujo, Backward bifurcation and control in transmission dynamics of arboviral diseases, Math. Biosc, 278 (2016) 100–129.

[2] H. Abboubakar, J.C. Kamgang, L.N. Nkamba, D. Tieudjo, Bifurcation thresholds and optimal control in transmission dynamics of arboviral diseases, J. Math. Biol, 107 (2017) 379–427.

[3] M.E. Alexander, C. Bowman, S.M. Moghadas, R. Summers, A.B. Gumel, B.M. Sahai, A Vaccination Model for Transmission Dynamics of Influenza, Siam J. Appl. Dyn. Syst, 10 (2004) 503–524.

[4] R. Anderson, R. May, Infectious disease of humans: Dynamics and control, Oxford university press, Oxford, UK, 1991.

[5] E.A. Bakare, A. Nwagwo, E. Danso-Addo, Optimal control analysis of an SIR epidemic model with constant recruitment, Int. J. Appl. Math, 3 (2014) 273–285.

[6] T. Berge, S. Bowong, J.M.S. Lubuma, Global stability of a two-patch cholera model with fast and slow transmissions, Math. Comp. Simul, 241 (2014) 317–331.

[7] Bhandare, G. Sudhakar, Biocontrol of V. cholorae using bacteriophages. Phd thesis, university of Nottingham, 2015.

[8] G. Birkhoff, G.C. Rota, Ordinary Differential Equations, 4th edition, John Wiley & Sons, Inc., New York,1989.

[9] M. Brigid, K.W. Matthe, Fillamentous phages linked to virulence of vibrio cholerae, Curr. Opi. Micro, 6 (2003) 35–42.

[10] C.C. Chavez, B. Song, Dynamical models of tuberculosis and their application, Math. Biosci. Eng, 12 (2004) 361–404.

[11] C.T. Codeco, Endemic and epidemic dynamics of cholera: the role of the aquatic reservoir, BMC. Infect. Dis, 1 (2001) 1–14.

[12] C. Yang, J. Wang, On the intrinsec dynamics of bacteria in waterborne infection, Math. Biosc, 296 (2018) 338–339.

[13] E. Dangbe, D. Irephan, A. Perasso, D. Bekolle, Mathematical modelling and numerical simulations of the infuence of hygiene and seasons on the spread of cholera, Math. Biosc, 296 (2018) 60–70.

[14] Y.M. Dessaleg, A.B. Gumel, Global asymptotic properties of an SEIRS model with multiple infectious stages. J. Math. Anal. Appl, 366 (2010) 202–217.

[15] S.M. Faruque, M. John, Phage-bacterial interactions in the evolution of toxigenic vibrio cholerae, Virulence, 42 (2012) 599–653.

[16] H.I. Fremann, S. Ruan, M. Tan, Uniform persistence and flows near a close positively invariant set. J. Diff. Equ, 4 (1994) 583-600.

[17] S.M. Garba, A.B. Gumel, M.R. AbuBakar, Backward bifurcations in dengue transmission dynamics, Math. Biosc, 215 (2008) 11–25.

[18] A.B. Gumel, Causes of backward bifurcations in some epidemiological models, J. Math. Anal. Appl, 395 (2012) 355–365.

[19] A.B. Gumel, B. Song, Existence of multistable equilibria for a multi-drug-resistant model of mycobacterium tuberculosis, Math. Biosc. Eng, 67 (2008) 437–455.

[20] B.R. Guttman Raya and Ekutter, Bacteriophage: Biology and application. CRC Press, USA (2005) 29–66.

[21] J. Gjorgjieva, K. Smith, G. Chowell, F. Sanchez, J. Snyder, C. Castillo-Chavez, The role of vaccination in the control of SARS, Math. Biosc. Eng, 2 (2005) 1–17.

[22] Harris, J.B. Larocque, R.C. Quedri, E.T. Ryan, Lancet, 379 (2012) 2466-2476.

[23] E. Harrison, M.A. Brockhurst, Ecological and Evolutionary Benefits of Temperate Phage: What Does or Doesn't Kill You Makes Stronger, Bioessays, 39 (2017) 01–12.

[24] P. Hyman, Phages for Phage Therapy: Isolation, Characterization, and Host Range Breadth, Pharmaceuticals (Basel), doi: 10.3390/ph12010035. (2019).

[25] J.C. Kamgang, G. Sallet, Computation of threshold conditions for epidemiological models and global stability of the disease-free equilibrium (DFE), Math. Biosc, 213 (2008) 1–12.

[26] Kbenesh, W. Blayneh, A.B. Gumel, S. Lenhart, T. Clayton, Backward Bifurcation and Optimal Control in Transmission Dynamics of West Nile Virus, Bull. Math. Biol, 72 (2010) 1006–1028.

[27] G.G. Kolaye, S. Bowong, R. Houe, M.A. Aziz-Alaoui, M. Cadivel, Mathematical assessment of the role of environmental factors on the dynamical transmission of cholera, Com. Non. Sci. Num. Sim, 67 (2019) 203–222.

[28] J.D. Kong, W. Davis, A.H. Wang, Dynamics of a Cholera Transmission Model with Immunological Threshold and Natural Phage Control in Reservoir, Bull. Math. Biol, 76 (2014) 2025–2051.

[29] S. Lakshmikantham, S. Leela, A.A Martynyk, stability analysis of non linear system, Marcel dekker, Inc, New York, Basel 1989.

[30] J.P. LaSalle, The stability of Dynamical systems, Regional conference series in applied Mathemetics, SIAM, Philadelphia 1976.

[31] J.P. LaSalle Stability theory for ordinary differential equations. J. Differ. Equ. 41 (1968) 57–65.

[32] S. Lenhart, J.T. Workman, Optimal Control Applied to Biological Models, Mathematical and Computational Biology Series, Chapman & Hall/CRM (2007).

[33] A.K. Misra, G. Alok, V. Ezio, Cholera dynamics with bacteriophage infection: A mathematical study, Chao. Sol. Frac, 91 (2016) 610–621.

[34] R.V. Miller, M. Day, Contribution, pseudlysogeny and starvation to phage ecology. Bact. Ecol. AST, UK Cambridge University Press (2008) 114–143.

[35] S.M. Moghadas, M.E. Alexander, Exogenous reinfection and resurgence of tuberculosis: A theoretical framwork, J. Biol. Syst, 12 (2004) 231–247.

[36] A. Mwasa, J.M. Tchuenche, Mathematical analysis of a cholera model with public healh intervention, BioSystems, 105 (3) (2011) 190–200.

[37] H.M. Ndongmo Teysta, B. Tsanou, S. Bowong, J. Lubuma, Bifurcation analysis of a phage bacteria interaction model with prophage induction, Math. Med. Biol. 00 (2020), 1–31.

[38] J.B.H. Njagarah, F. Nyabadza, A metapopulation model for cholera transmission dynamics between communities linked by migration, Appl. Math. Comp, 241 (2014) 317–331.

[39] J.B.H. Njagarah, F. Nyabadza, Modelling Optimal Control of Cholera in Communities Linked by Migration, Comput. Math. Method. Med. 2015, Article ID 898264, 12 pages.

[40] N. Plaza, D. Castillo, D.P Reytor, G. Higuera, K. Garcia, R. Bastias, Bacteriophages in the control of pathogenic vibrios, Elec. J. Biotech, 31 (2018) 24–33.

[41] P. Van Den Driessche, J. Wathmough, Reproduction number and subtrheshold endemic equilibria for compartemental models of disease transmission, Math. Biosc, 180 (2002) 29–48.

[42] C.J. Ray, S. Mariano, I.B. Hogue, D.E. Kirschner, A methodology for performing global uncertainty and sensitivity analysis in system biology, J. Theor. Biol, 254 (2008) 178–196. 4

[43] F. Richard, Medical Microbiology: A Guide to Microbial Infections: Pathogensis, Immunity, Laboratory Diagnosis and Control,Churchill Livingstone, 16 edition , 2002.

[44] C.A. Roberto, H.M. Yang, L. Esteva, Optimal control of Aedes aegypti mosquitoes by the sterile insect technique and insecticide, Math. Biosc, 223 (2010) 12–23.

[45] Z. Shuiai, P. Van den Driessche, Global stability of infectious disease models using Lyapunov, Siam J. Appl. Math 73 (2013) 1513–1532.

[46] S.L. Díaz-Muñoz, B. Koskella, Bacteria-Phage Interactions in Natural Environments, Adv. Appl. Microbiol 89 (2014) 135–83.

[47] O.S. Sisodiya, O.P. Misra, J. Dhar, Dynamics of cholera epidemics with impulsive vaccination and desinfection, Math. Biosc, 298 (2018) 46–57.

[48] O.S. Sisodiya, O. P. Misra, J. Dhar, Pathogen Induced Infection and Its Control by Vaccination: A Mathematical Model for Cholera Disease, Int. J. Appl. Comp. Math, 11 (2018) 4–74.

[49] H.L. Smith, Models of virulent phage growth with application to phage therapy, Siam J. Appl. Math, 68 (2008) 1717–1737.

[50] Sukhita, W. Vidurupola, Analysis of deterministic and stochastic mathematical models with resistant bacteria and bacteria debris for bacteriophage dynamics, Appl. Math. Comp, 316 (2018) 215–228.

[51] W. Xueyung, W. Jin, Modelling the within-host dynamics of cholera: Bacteria-viral interaction. J.Biol.Dync 11(2017) 484–501.

[52] M.B. Yaghoub, R. Gautam , Z. Shuai, P. van den Driessche, R. Ivanek, Reproduction numbers for infections with free-living pathogens growing in the environment, J. Biol. Dyn, 6 (2012) 923–940.

[53] C. Yang, J. Wang, On the intrinsic dynamics of bacteria in waterborne infections, Math.Biosc, 296 (2018) 71–81.

[54] C. Yang, D. Posny, F. Bao, J. Wang, A multi-scale cholera model linking between-host and within-host dynamics, Int.J. Biomath, 3 (2018) 18–34.

[55] X. Yang, L. Chen, J. Chen, permanence and positive periodic solution for the single-species nonautonomous delay diffuse models, Comp. Math. Appl, 32 (1996) 109–116.

[56] CDC, Information for public health and medical proffesionals, Center of disease control and prevention, https://www.cdc.gov/cholera/healthprofessionals.html, last access 12 February 2020.

[57] GBD Mortality and causes of death collaborators "Global, regional and national life expectancy, all-cause mortality, and cause-specific mortality for 249 causes of death, 1980-2015: a symetric analysis for the global burden of disease study 2015" Lancet, 388 (10053): 1459–1544.